# Conditional Coverage Estimation for High-Quality Prediction Intervals

**Ziyi Huang**[1], **Henry Lam**[1], **Haofeng Zhang**[1]

[1]School of Engineering and Applied Science, Columbia University, New York, NY 10027, USA;

zh2354@columbia.edu, khl2114@columbia.edu, hz2553@columbia.edu

**Abstract**

Deep learning has been recently studied to generate high-quality prediction intervals (PIs) for uncertainty quantification in regression tasks, including recent applications in simulation metamodeling. The high-quality criterion requires PIs to be as narrow as possible, whilst maintaining a pre-specified level of data (marginal) coverage. However, most existing works for high-quality PIs lack accurate information on conditional coverage, which may cause unreliable predictions if it is significantly smaller than the marginal coverage. To address this problem, we propose an end-to-end framework which could output high-quality PIs and simultaneously provide their conditional coverage estimation. In doing so, we design a new loss function that is both easy-to-implement and theoretically justified via an exponential concentration bound. Our evaluation on real-world benchmark datasets and synthetic examples shows that our approach not only achieves competitive results on high-quality PIs in terms of average PI width, but also accurately estimates conditional coverage information that is useful in assessing model uncertainty.

**Keywords:** Uncertainty quantification, prediction intervals, conditional coverage, neural networks, calibration error

## 1 Introduction

Prediction interval (PI) is poised to play an increasingly prominent role in uncertainty quantification for regression tasks (Khosravi et al. , 2010, 2011; Galván et al. , 2017; Rosenfeld et al. , 2018; Tagasovska and Lopez-Paz , 2018, 2019; Romano et al. , 2019; Wang et al. , 2019; Kivaranovic et al. , 2020). Recently, it has also been used in simulation metamodeling Lam and Zhang (2021, 2022) in the spirit of the widely used stochastic kriging and Gaussian process methodologies Ankenman et al. (2010); Barton and Meckesheimer (2006); Staum (2009). A *high-quality* PI should be as narrow as possible, whilst maintaining a pre-specified level of data coverage or marginal coverage (Pearce et al. , 2018; Zhu et al. , 2019). Compared with PIs obtained based on coverage-only consideration, the "high-quality" criterion is beneficial in balancing between marginal coverage probability and interval width. However, the conditional coverage given a feature, which is critical for making reliable context-based decisions, is unassessed and missing in most existing works on high-quality PIs. In the presence of heteroskedasticity and model misspecification, the marginal coverage can be very different from the conditional coverage at a given point, which affects the downstream decision-making task that relies on the uncertainty information provided by the PI. Our main goal is to meaningfully incorporate and assess conditional coverages in high-quality PIs.

Conditional coverage estimation is challenging for two reasons. First is that the natural evaluation metric of *conditional coverage error*, an $L^p$ distance between the estimated and ground-truth conditional coverages, is difficult to compute as it requires obtaining the conditional probability given feature $x$, which is arguably as challenging as the regression problem itself. Our first goal in this paper is to address this issue by developing a new metric called *calibration-based conditional coverage error* for conditional coverage estimation measurement. Our approach is inspired from the calibration notion in classification (Guo et al. , 2017). The basic idea is to relax conditional coverage at any given point to being averaged over all points that bear the same estimated value. An estimator satisfying the relaxed property is regarded as well-calibrated. In regression, calibration-based conditional coverage error provides a middle ground between the enforcement of marginal coverage (lacking any conditional information) and conditional coverage (computationally intractable). Compared with conditional coverage, this middle-ground metric can be viewed as a "dimension reduction" of the conditioning variable from the original sample space to the space $[0, 1]$, so that we can easily discretize to compute the empirical metric values.

The second challenge is the discontinuity in the above metrics that hinders efficient training of PIs that are both high-quality and possess reliable conditional coverage information. To address this, we design a new loss function based on a combination of the high-quality criterion and a *coverage assessment loss*. The latter can be flexibly added as a separate module to any neural network (NN) used to train PIs. It is based on an empirical version of a tight upper bound on the coverage error in terms of a Kullback–Leibler (KL) divergence, which can be readily employed for running gradient descent. We theoretically show how training with our proposed loss function attains this upper-bounding value via a concentration bound. We also demonstrate the empirical performance of our approach in terms of PI quality and conditional coverage assessment compared with benchmark methods.

We summarize our contributions as follows:

1. We identify the conditional coverage estimation problem as a new challenge for high-quality PIs and introduce a new evaluation metric for coverage estimation.

2. We propose an end-to-end algorithm that can simultaneously construct high-quality PIs and generate conditional coverage estimates. In addition, we provide theoretical justifications on the effectiveness of our algorithm by developing concentration bounds relating the coverage assessment loss and conditional coverage error.

3. By evaluating on benchmark datasets and synthetic examples, we empirically demonstrate that our approach achieves high performance on conditional coverage estimation without penalizing the performance on high-quality PI generation.

## 2 Evaluating Conditional Coverage for High-Quality PIs

Let $X \in \mathcal{X}$ and $Y \in \mathcal{Y} \subset \mathbb{R}$ be random variables denoting the input feature and label, where the pair $(X, Y)$ follows an (unknown) ground-truth joint distribution $\pi(X, Y)$. Let $\pi(Y|X)$ be the conditional distribution of $Y$ given $X$. Let $\pi(X)$ be the marginal distribution of $X$. We are given the training data $\mathcal{D} := \{(x_i, y_i),\ i = 1, 2, \cdots, n\}$ where $(x_i, y_i)$ are i.i.d. realizations of random variables $(X, Y)$. Here, $(x_i, y_i)$ could denote supervised real data. It can also denote, in the simulation context, a simulation model output $y_i$ given the design point $x_i$.

A PI refers to an interval $[L(x), U(x)]$ where $L$, $U$ are two functions mapping from $\mathcal{X}$ to $\mathcal{Y}$ trained on the data $\mathcal{D}$. $[L(x), U(x)]$ is called a PI at *prediction level* $1 - \alpha$ $(0 \leq \alpha \leq 1)$ if its *marginal coverage* is not less than $1 - \alpha$, i.e., $\mathbb{P}[Y \in [L(X), U(X)] | L, U] \geq 1 - \alpha$ where $\mathbb{P}$ is with respect to a new test point $(X, Y) \sim \pi(X, Y)$.

We say that $[L(x), U(x)]$ is of high-quality if its marginal coverage attains a pre-specified target prediction level and has a short width on average. In particular, a best-quality PI at prediction level $1 - \alpha$ is an optimal solution to the following constrained optimization problem:

$$\min_{L,U} \mathbb{E}[U(X) - L(X)],$$
$$\text{subject to } \ \mathbb{P}[Y \in [L(X), U(X)] | L, U] \geq 1 - \alpha. \tag{1}$$

The high-quality criterion has been widely adopted in previous work Khosravi et al. (2010, 2011); Galván et al. (2017); Pearce et al. (2018); Rosenfeld et al. (2018); Zhu et al. (2019); Chen et al. (2021). However, this criterion alone may fail to carry important model uncertainty information at specific test points. To illustrate this statement, consider a simple example where $x \sim \text{Uniform}[0, 1]$, $y = 0$ for $x \in [0, 0.95]$ and $y|x \sim \text{Uniform}[0, 1]$ for $x \in (0.95, 1]$. Then according to Equation 1, a best-quality 95% PI is precisely $L(x) = U(x) = 0$ for all $x \in [0, 1]$. This PI has nonconstant "conditional" coverage if we condition at different input points (1 for $x \in [0, 0.95]$ and 0 for $x \in (0.95, 1]$), and can deviate significantly from the overall marginal coverage 95%. Therefore, it is sometimes important to obtain conditional coverage information, especially when the conditional coverage at some input points differs a lot from the marginal coverage. This simple example highlights the need to obtain conditional coverage information.

To mitigate the drawback of the high-quality criterion, we define:

**Definition 1** (Conditional Coverage and Its Estimator)**.** *The (ground-truth) conditional coverage associated with a PI* $[L(x), U(x)]$ *is defined as* $A(x) := \mathbb{P}[Y \in [L(X), U(X)] | L, U, X = x]$ *for any* $x \in \mathcal{X}$, *where* $\mathbb{P}$ *is taken with respect to* $\pi(Y|X = x)$. *For a (conditional) coverage estimator* $\hat{P}$, *which is a measurable function from* $\mathcal{X}$ *to* $[0, 1]$, *we define its* $L^p$ *conditional coverage error* ($\widetilde{CE}_p$) *as*

$$\widetilde{CE}_p := \left\| A(X) - \hat{P}(X) \right\|_{L^p(\mathcal{X})}$$

*where the* $L^p$*-norm is taken with respect to the randomness of* $X$ $(1 \leq p \leq +\infty)$*.*

Note that evaluating $\widetilde{CE}_p$ relies on approximating the conditional coverage $A(x)$, which can be as challenging as the original prediction problem. To address this, we leverage the similarity of estimating $A(x)$ to generating prediction probabilities in binary classification, which motivates us to borrow the notion of calibration in classification. This idea is based on a relaxed error criterion by looking at the conditional coverage among all points that bear the same coverage estimator value, instead of conditioning at any given point. The resulting error metric then only relies on probabilities conditioned on variables in a much lower-dimensional space $[0, 1]$ than $\mathcal{X}$. To explain concretely, we introduce a "perfect-calibrated coverage estimator" as:

**Definition 2** (Perfect Calibration). *A coverage estimator $\hat{P}$ is called a perfect-calibrated coverage estimator associated with $[L(x), U(x)]$ if it satisfies*

$$\hat{P}(x) = \mathbb{P}[Y \in [L(X), U(X)]|L, U, \hat{P}(X) = \hat{P}(x)], \tag{2}$$

*for a.e. $\hat{P}(x) \in [0, 1]$ where a.e. is with respect to the probability measure on $[0, 1]$ induced by the random variable $\hat{P}(X)$.*

Equation 2 means that the "average" coverage of the PI restricted on the subset $\{x \in \mathcal{X} : \hat{P}(x) = p\}$ should be precisely $p$ (where the "average" coverage is the average of all the conditional coverage $A(x)$ on the subset $\{x \in \mathcal{X} : \hat{P}(x) = p\}$, with respect to the distribution $\pi(X)$ conditional on the subset $\{x \in \mathcal{X} : \hat{P}(x) = p\}$). Corresponding to Definition 2, we define:

**Definition 3** (Calibration-based Error). *An $L^p$ ($1 \leq p \leq +\infty$) calibration-based conditional coverage error, or coverage error for short ($CE_p$), of a coverage estimator $\hat{P}$ is:*

$$CE_p := \left\| \mathbb{P}[Y \in [L(X), U(X)]|L, U, \hat{P}(X)] - \hat{P}(X) \right\|_{L^p(\mathcal{X})} \tag{3}$$

*where the $L^p$-norm is taken with respect to the randomness of $\hat{P}(X)$.*

In the above definition the conditional probability $\mathbb{P}[Y \in [L(X), U(X)]|L, U, \hat{P}(X)]$ is a measurable function of random variable $\hat{P}(X)$, say $\gamma(\hat{P}(X))$. By a change of variable,

$$CE_p^p := \left\| \gamma(\hat{P}(X)) - \hat{P}(X) \right\|_{L^p(\mathcal{X})}^p \tag{4}$$

$$= \int_0^1 |\gamma(t) - t|^p dF_{\hat{P}(X)}(t) \tag{5}$$

where $F_{\hat{P}(X)}$ is a probability distribution of $\hat{P}(X)$ on $[0, 1]$. Here, $CE_p$ only requires estimating $\gamma(t)$ for $t \in [0, 1]$, which can be done easily by discretizing $[0, 1]$ for empirical calculation. To do this, we first construct a discrete version of (2) and then introduce an empirical counterpart of $CE_p$ (3), which we refer to as $L^p$ empirical calibration-based conditional coverage error $ECE_p$. The ideas behind these are natural extensions of the classification case (Guo et al. , 2017; Kull , 2019; Kumar , 2019; Nixon et al. , 2019) into PIs.

We consider the following partition $\Delta$ of $[0, 1]$. Let $[0, 1]$ be divided into $M$ intervals $I_m = (a_{m-1}, a_m]$ ($m = 1, \cdots, M$) where $0 = a_0 \leq a_1 \leq \cdots \leq a_M = 1$. Let $B_m = \{i = 1, \cdots, n : \hat{P}(x_i) \in I_m\}$, i.e., the set (bin) of indices $i$ of samples whose coverage estimator $\hat{P}(x_i)$ falls into the interval $I_m$. Note that coverage estimations that are close to each other will fall into the same interval. The coverage probability (i.e., the proportion of successful coverage) in $B_m$ is defined as:

$$CP(B_m) = \frac{1}{|B_m|} \sum_{i \in B_m} \mathbf{1}_{y_i \in [L(x_i), U(x_i)]}. \quad (6)$$

The average coverage estimation in $B_m$ is defined as:

$$AC(B_m) = \frac{1}{|B_m|} \sum_{i \in B_m} \hat{P}(x_i) \quad (7)$$

where $\hat{P}(x_i)$ is the coverage estimator for sample $x_i$. $CP(B_m)$ and $AC(B_m)$ approximate the left and right hand sides of (2) respectively in the interval $I_m$. A perfect-calibrated coverage estimator should satisfy $CP(B_m) = AC(B_m)$ for all $m \in \{1, \cdots, M\}$. The diagram of $CP(B_m)$ versus $AC(B_m)$ for all $m \in \{1, \cdots, M\}$ is called the reliability diagram in some literature (Guo et al. , 2017).

Based on the partition $\Delta$, we can introduce an empirical version of $CE_p$ (which we refer to as $ECE_p$) as:

**Definition 4.** *The $L^p$ empirical calibration-based conditional coverage error ($ECE_p$) of a coverage estimator $\hat{P}$ is defined as*

$$ECE_p = \left\| (CP(B_{m(i)}) - AC(B_{m(i)}))_{i=1,2,\cdots,n} \right\|_{l^p}. \quad (8)$$

*where the $l^p$ is the standard p-norm in $\mathbb{R}^n$ and $B_{m(i)}$ is the bin containing sample i.*

Equivalently,

$$ECE_p = \left( \sum_{m=1}^{M} \frac{|B_m|}{n} |CP(B_m) - AC(B_m)|^p \right)^{\frac{1}{p}}$$

for $1 \leq p < +\infty$, and

$$ECE_\infty = \max_{m=1,2,\cdots,M} |CP(B_m) - AC(B_m)|.$$

A calibration-based error $CE_p$ provides a middle ground between the enforcement of marginal coverage and conditional coverage. The ground-truth conditional coverage is perfectly calibrated, but not vice versa. However, if we enforce the perfect calibration criterion for a coverage estimator to hold when restricted to any positive-probability measurable subset in $\mathcal{X}$, then the choice of the estimator will reduce uniquely to the conditional coverage. More formally,

**Definition 5.** *A coverage estimator $\hat{P}$ is called a perfect-calibrated coverage estimator on a measurable subset $\mathcal{S} \subset \mathcal{X}$ with $\mathbb{P}(\mathcal{S}) > 0$ associated with $[L(x), U(x)]$ if it satisfies*

$$\hat{P}(x) = \mathbb{P}[Y \in [L(X), U(X)] | L, U, \hat{P}(X) = \hat{P}(x), X \in \mathcal{S}] \quad (9)$$

*for a.e. $\hat{P}(x) \in [0,1]$ where a.e. is with respect to the probability measure on $[0,1]$ induced by the random variable $\hat{P}(X|_{\mathcal{S}})$. Note that the conditional probability space is standard: $(\mathcal{S}, \mathcal{F}_{\mathcal{S}} := \{A \cap \mathcal{S} : A \in \mathcal{F}\}, \mathbb{P}_{\mathcal{S}}(A \cap \mathcal{S}) := \mathbb{P}(A|\mathcal{S}))$.*

**Lemma 1.** *(a) A coverage estimator is the conditional coverage if and only if it is a perfect-calibrated coverage estimator on any positive-probability measurable subset $\mathcal{S}$ of $\mathcal{X}$.*
*(b) Suppose $\hat{P}$ is a perfect-calibrated coverage estimator on two disjoint positive-probability measurable subsets $\mathcal{S}_1$, $\mathcal{S}_2$. Then $\hat{P}$ is a perfect-calibrated coverage estimator on $\mathcal{S}_1 \cup \mathcal{S}_2$.*

More details can be found in Appendix A. In the sense of Lemma 1(a), $CE_p$ is an error metric that is a natural relaxation of $\widetilde{CE}_p$, and although less precise, $CE_p$ is computationally much more tractable than $\widetilde{CE}_p$.

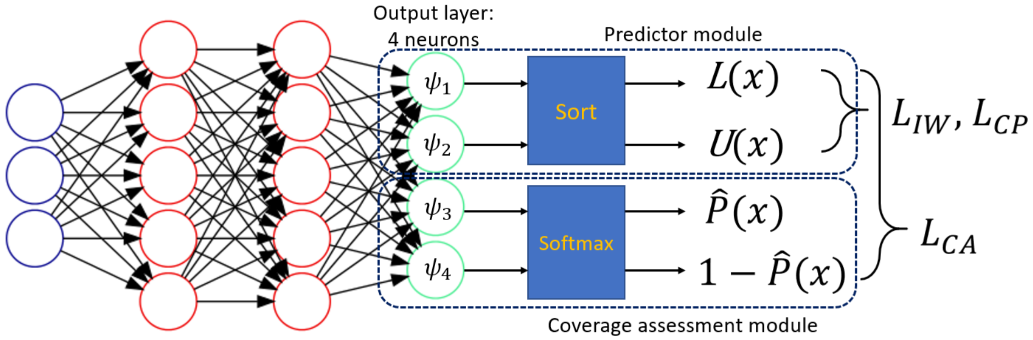

Figure 1: The framework of our proposed coverage assessment network (CaNet).

We will use $ECE_1$ as the primary evaluation metric to measure the quality of a coverage estimator. A high $ECE_1$ value of a coverage estimator indicates an unreliable coverage estimation while a small $ECE_1$ value indicates that the coverage estimator is close to the perfect-calibrated property. Ideally, an effective algorithm should output a coverage estimator with a small $ECE_1$ value.

## 3 Neural Network for Conditional Coverage

We propose a novel end-to-end algorithm, named coverage assessment network (CaNet), to simultaneously generate a coverage estimator along with the high-quality PI. As illustrated in Figure 1, our CaNet takes any input data $x$ as its input layer (the leftmost layer in Figure 1), feeds $x$ in the forward direction through the network, and obtains four output values $(\psi_1(x), \psi_2(x), \psi_3(x), \psi_4(x))$ in the output layer. Then these output values are used in two major modules in our CaNet: (1) **predictor module** and (2) **coverage assessment module** (Ca-Module). The PI predictor module sorts the two outputs $(\psi_1(x), \psi_2(x))$ to provide the upper and lower bound of the estimated PIs. Meanwhile, the Ca-Module is added to the output layer to access the conditional coverage information of PIs from the predictor module. Our model is jointly optimized by three loss functions: coverage assessment loss $L_{CA}$, intervals width loss $L_{IW}$, and coverage probability loss $L_{CP}$. Benefiting from these powerful modules, the CaNet can generate and validate the coverage estimator at the same time without any requirement for further post-processing steps. In addition, we propose a novel deep ensemble technique, suitably designed for our setting, that can improve the performance of both the predictor module and the coverage assessment module.

### 3.1 Coverage Assessment Module

Our Ca-Module consists of two neurons $(\psi_3(x), \psi_4(x))$ fully connected to the last hidden layer to estimate the conditional coverage. After letting $(\psi_3(x), \psi_4(x))$ pass through the softmax activation function, it outputs a two-point probability distribution $(\hat{P}(x), 1-\hat{P}(x))$

where $\hat{P}(x)$ is viewed as the coverage estimator of the PI from the predictor module. Our Ca-Module can be easily integrated into the output layer of deep neural networks to estimate their conditional coverage.

### 3.2 Loss Function Design and Tuning Procedure

Our loss function is a sum of the *predictor loss* and the *coverage loss*. The predictor loss aims to narrow the prediction intervals as much as possible, while maintaining a specified marginal coverage of data. Inspired by Khosravi et al. (2010, 2011); Pearce et al. (2018); Rosenfeld et al. (2018), our predictor loss is formed by the sum of interval width (IW) loss $L_{IW}$ and coverage probability (CP) loss $L_{CP}$:

$$L_{IW} = \frac{1}{n}\sum_{i=1}^{n}(U(x_i) - L(x_i)), \tag{10}$$

$$L_{CP} = \frac{1}{n}\sum_{i=1}^{n}\tilde{k}_i, \quad CP = \frac{1}{n}\sum_{i=1}^{n}k_i, \tag{11}$$

where $k_i$ indicates whether each data point has been captured by the PIs: $k_i = 1$ if $L(x_i) \leq y_i \leq U(x_i)$ and $k_i = 0$ otherwise. $\tilde{k}_i$ is a soft version of $k_i$, which is defined as: $\tilde{k}_i := \sigma(\lambda_3(U(x_i)-y_i))\cdot\sigma(\lambda_3(y_i-L(x_i)))$, where $\lambda_3 \geq 0$ is a tunable parameter and $\sigma(t) := \frac{1}{1+e^{-t}}$ is the sigmoid function. Therefore, $L_{CP}$ is a soft version of $CP$ that can be used for gradient descent. Associated with the Ca-Module, we introduce a coverage assessment loss $L_{CA}$ to estimate the conditional coverage:

$$L_{CA} = -\frac{1}{n}\sum_{i=1}^{n}\Big(k_i\log(\hat{P}(x_i)) + (1-k_i)\log(1-\hat{P}(x_i))\Big).$$

We will show in Section 4 that the expectation of coverage assessment loss $L_{CA}$ provides an upper bound for both the conditional coverage error (Definition 1) and calibration-based conditional coverage error (Definition 3). Hence, minimizing $L_{CA}$ contributes to the recovery of the conditional coverage. In order to run gradient-based methods, we replace the discrete indicator $(k_i, 1-k_i)$ in $L_{CA}$ with its soft version $(\tilde{k}_i, 1-\tilde{k}_i)$:

$$\tilde{L}_{CA} = -\frac{1}{n}\sum_{i=1}^{n}\Big(\tilde{k}_i\log(\hat{P}(x_i)) + (1-\tilde{k}_i)\log(1-\hat{P}(x_i))\Big).$$

Our total loss function for the CaNet is defined as:

$$\text{Total Loss} = L_{IW} + \lambda_1(1-L_{CP}) + \lambda_2\tilde{L}_{CA} \tag{12}$$

where $\lambda_1 \geq 0$, $\lambda_2 \geq 0$ are tunable parameters. We propose an easy-to-implement yet effective tuning procedure, Algorithm 1, to pick up these parameters.

### 3.3 Deep Ensembles

Following previous research (Lee et al. , 2015; Lakshminarayanan , 2017; Pearce et al. , 2018; Fort et al. , 2019; Ovadia et al. , 2019; Gustafsson et al. , 2020; Pearce et al. , 2020), we apply the deep ensemble technique to provide more robust and better results. During the training period, with the same hyperparameters $\lambda_i, i = 1, 2, 3$, $m$ networks are trained with different initializations. The prediction results from $i$-th network are denoted as: $([L_i(x), U_i(x)], \hat{P}_i(x), 1 -$

**Algorithm 1** Tuning algorithm

**Goal**: Tune hyperparameters $\lambda_1$, $\lambda_2$, and $\lambda_3$;

**Input**: Prediction level $1-\alpha$, training dataset $\mathcal{D}$, validation dataset $\mathcal{D}'$;

**Procedure**: Let the coverage probability $CP_{\mathcal{D}'}$ and the average coverage estimation $AC_{\mathcal{D}'}$ on $\mathcal{D}'$ be

$$CP_{\mathcal{D}'} = \frac{1}{|\mathcal{D}'|}\sum_{i\in\mathcal{D}'} \mathbf{1}_{y_i\in[L(x_i),U(x_i)]},$$

$$AC_{\mathcal{D}'} = \frac{1}{|\mathcal{D}'|}\sum_{i\in\mathcal{D}'} \hat{P}(x_i).$$

where $([L(x),U(x)],\hat{P}(x))$ are prediction results from the deep ensemble.

(1) Initialize $\lambda_i$ $(i=1,2,3)$ so that $CP_{\mathcal{D}'}$ is nontrivial, i.e., not (almost) 0 or 1.

(2) While $CP_{\mathcal{D}'}$ is nontrivial: tune $\lambda_2$ and $\lambda_3$ so that $|CP_{\mathcal{D}'} - AC_{\mathcal{D}'}| \le \epsilon$ (e.g., $\epsilon = 1\%$.)

(3) Otherwise tune $\lambda_1$ such that $CP_{\mathcal{D}'}$ is nontrivial. Do step 2 again until we find $\lambda_2$ and $\lambda_3$.

(4) Tune $\lambda_1$ such that $CP_{\mathcal{D}'} > 1-\alpha$ where $\lambda_2$ and $\lambda_3$ are fixed from (3).

**Output**: $\lambda_1$, $\lambda_2$, and $\lambda_3$.

$\hat{P}_i(x)$). Finally, the output from CaNet is:

$$\begin{array}{lcl} \textit{Lower bound} & \bar{L} & := \sum_{i=1}^{m}\frac{1}{m}L_i, \\ \textit{Upper bound} & \bar{U} & := \sum_{i=1}^{m}\frac{1}{m}U_i, \\ \textit{Coverage estimator} & \bar{\hat{P}} & := \sum_{i=1}^{m}\frac{1}{m}\hat{P}_i. \end{array} \tag{13}$$

# 4 Theoretical Analysis

In this section, we provide theoretical insights about the coverage assessment loss $L_{CA}$ in our approach. We show that minimizing $L_{CA}$ is equivalent to minimizing a tight upper bound of the conditional coverage error with high probability and thus contributes to reducing the conditional coverage error of a coverage estimator. This theoretical analysis consists of two steps. First, we show that both $CE_p$ and $\widetilde{CE}_p$ are bounded above by the expectation of a Kull-back–Leibler divergence-type risk $K_1(X)$. Second, we establish the tail bound of the generalization error $\mathbb{E}[K_1(X)]$ and its empirical counterpart which is exactly $L_{CA}$. We will show that the generalization bound holds uniformly for any tuple of the joint output functions $(L(x),U(x),\hat{P}(x),1-\hat{P}(x))$ generated by our CaNet. Because multiple hypothesis classes beyond $(L(x),U(x),\hat{P}(x),1-\hat{P}(x))$ are involved in $L_{CA}$, more effort is required to build the connection among them to derive the generalization bound.

**Theorem 1.** *Let* $A(x) := \mathbb{P}[Y \in [L(X),U(X)]|L,U,X = x]$ *be the conditional coverage in Definition 1. Let* $K(x) := A(x)\log\left(\frac{A(x)}{\hat{P}(x)}\right) + (1-A(x))\log\left(\frac{1-A(x)}{1-\hat{P}(x)}\right)$. *Then*

$$CE_p \le \widetilde{CE}_p \le \left(\frac{1}{2}\mathbb{E}[K(X)]\right)^{\alpha_p/2}, \forall 1 \le p \le +\infty$$

*where* $\alpha_p = 1, \forall 1 \le p \le 2$ *and* $\alpha_p = \frac{2}{p}, \forall 2 \le p \le +\infty$. *Moreover, the inequality is attainable if, e.g.,* $\hat{P}(x)$ *equals the conditional coverage* $A(x)$.

From Theorem 1, we see that minimizing $\mathbb{E}[K(x)]$ is equivalent to minimizing a tight upper bound for the coverage error. For every $x$, $K(x)$ is the Kullback–Leibler divergence between the distributions represented by $(\hat{P}(x), 1-\hat{P}(x))$ and $(A(x), 1-A(x))$. $K(x) = K_0(x) + K_1(x)$, where $K_0(x) = A(x)\log(A(x)) + (1-A(x))\log(1-A(x))$ and $K_1(x) = -A(x)\log(\hat{P}(x)) - (1-A(x))\log(1-\hat{P}(x))$. Minimizing $\mathbb{E}[K(X)]$ over $\hat{P}$ is equivalent to minimizing $\mathbb{E}[K_1(X)]$. The type of results in Theorem 1 that bounds an $L^p$ conditional coverage error via a Kullback-Leibler-type error is new as far as we know. Next, to show $L_{CA}$ approximates $\mathbb{E}[K_1(X)]$, we need the following assumptions:

**Assumption 1.** *The four classes of functions $([L(x), U(x)], \hat{P}(x), 1-\hat{P}(x))$ output by the neural network (NN) in Figure 1 have finite VC dimensions, say they are bounded above by $V_0$.*

Assumption 1 holds for a wide range of NNs (e.g., Theorem 8.14 in Anthony and Bartlett (1999), Theorem 7 in Bartlett et al. (2019)). In particular, it holds for the one we adopt in the experiments (where we use the ReLU-activated NN to construct $\psi_i$, $i = 1, 2, 3, 4$; see Section 5):

**Theorem 2.** *Suppose $\psi_i, i = 1, 2, 3, 4$ are the pre-activated output neurons of the NN in Figure 1 using the ReLU activation function. Then Assumption 1 holds. Moreover, suppose the NN has $W$ parameters and $U$ computation units (nodes). Then $V_0 = O(WU)$.*

**Assumption 2.** *There exists a constant $M < +\infty$ such that $|\log(\hat{P}(x))| \leq M$, $|\log(1-\hat{P}(x))| \leq M$ for all $x$ and $\hat{P}$.*

This is a natural assumption in practice because $\log(\hat{P}(x))$ and $\log(1-\hat{P}(x))$ are replaced by $\log(\hat{P}(x)+\epsilon)$ and $\log(1-\hat{P}(x)+\epsilon)$ respectively to avoid explosion when implementing the algorithm. In particular, in our experiments in Section 5, $\epsilon = 0.1^6$ and thus $M = 14$. Let

$$\mathcal{F} = \{f(x,y) = I_{y\in[L(x),U(x)]} : \\ L, U \text{ are output by the NN}\},$$

$$\mathcal{G} = \{\hat{P}(x) : \hat{P} \text{ is output by the NN}\}.$$

**Theorem 3.** *Suppose Assumptions 1 and 2 hold. The training data $\mathcal{D} = \{(x_i, y_i),\ i = 1, 2, \cdots, n\}$ where $(x_i, y_i)$ are i.i.d. samples $\sim \pi$. Recall that the (hard) coverage estimator assessment loss is $L_{CA} = -\frac{1}{n}\sum_{i=1}^{n} \Big(f(x_i,y_i)\log(\hat{P}(x_i)) + (1-f(x_i,y_i))\log(1-\hat{P}(x_i))\Big)$. Then for any $t > 0$, we have*

$$\mathbb{P}\left(\sup_{f\in\mathcal{F},\hat{P}\in\mathcal{G}} |L_{CA} - \mathbb{E}[K_1(X)]| \geq t\right) \leq C^* e^{-\frac{nt^2}{16M^2}}.$$

*where $C^*$ only depends on $V_0$ in Assumption 1.*

Theorem 3 shows that the coverage assessment loss approximates $\mathbb{E}[K_1(x)]$ well with an exponential tail bound. The difficulty in analyzing Theorem 3 lies in the fact that the hypothesis classes in Assumption 1 (which are constructed by the NN) are different from the hypothesis class used in $L_{CA}$. To overcome this difficulty, we use the theory of VC-subgraph classes to connect the VC dimension among multiple hypothesis classes, including the class of $\psi_i$, the four classes of output functions, and $\mathcal{F}$, $\log \mathcal{G}$. Then we establish the covering number bound for the class $\mathcal{F}$ and $\log \mathcal{G}$, and finally prove Theorem 3. To conclude, minimizing $\mathbb{E}[K_1(X)]$ over $\hat{P}$ is equivalent to minimizing $\mathbb{E}[K(X)]$, which in turn is minimizing a tight upper bound for the coverage assessment loss. Our coverage assessment loss empirically approximates $\mathbb{E}[K_1(X)]$ well, so that its minimization can ultimately help to reduce the conditional coverage error.

## 5 Experiments

**Experimental Setup.** We empirically verify the effectiveness of our proposed CaNet on both synthetic examples and benchmark regression datasets. These datasets have been widely used for the evaluation of methods in regression tasks (Hernández-Lobato and Adams , 2015; Gal and Ghahramani , 2016; Lakshminarayanan , 2017; Rosenfeld et al. , 2018; Pearce et al. , 2018; Zhu et al. , 2019). In addition, we adopt the same experimental procedure in Pearce et al. (2018) for data normalization and dataset splitting. To avoid overfitting, we apply a simple network architecture with only 2 hidden layers and each hidden layer has 64 neurons. For each hidden layer, the ReLU activation function is applied to capture the non-linear features. We empirically set the ensemble number $m$ to 5, as the smallest number leading to a stable prediction results. Please refer to Appendix D for implementation details, including those for baseline algorithms.

**Evaluation Metrics.** To evaluate the conditional coverage estimation of our CaNet, we examine the quality of our Ca-Module measured by the empirical coverage error $ECE_1$ over a partition $\Delta$. $\Delta$ is constructed by equally dividing the width of $[0,1]$ into $M$ sub-intervals. The value of $M$ depends on the size of the dataset, which is determined by the following strategy: $M = \min\{\lfloor \text{the number of data in validation}/50 \rfloor + 1, 20\}$. In addition, we also report the $IW$ and $CP$, where $IW = \frac{1}{n}\sum_{i=1}^{n}(U(x_i) - L(x_i))$ (Equation 10) and $CP = \frac{1}{n}\sum_{i=1}^{n} k_i$, (Equation 11) to show the effectiveness of our predictor module under the high-quality criteria. Thanks to the deep ensemble technique (Section 3.3), our experimental results are robust and stable among multiple experimental repetitions with a standard deviation typically less than 2%. Therefore, we only report the mean value.

### 5.1 Conditional Coverage on Synthetic Examples

In this section, we conduct a series of experiments on synthetic examples to directly compare our prediction results with the ground-truth conditional coverage. In these examples, the conditional coverage can be analytically calculated under the known data distribution. Figure 2 compares the conditional coverage with our predicted coverage under the following settings: $x \sim \text{Uniform}[-2,2]$ and $y|x$ is drawn from $f_i(x) = \frac{1}{3}\sin(x) + \varepsilon_i(x), \; x \in [-2,2]$ where

$$\varepsilon_1(x) = 0.1 \times N(0,1),$$
$$\varepsilon_2(x) = 0.1|x| \times N(0,1),$$
$$\varepsilon_3(x) = 0.1|x| \times t_4.$$

$N(0,1)$ is the standard Gaussian variable and $t_4$ is the standard $t$ random variable with 4 degrees of freedom. Then, the conditional coverage in Definition 1 can be analytically calculated as:

$$\begin{aligned}&\mathbb{P}[Y \in [L(X), U(X)] | L, U, X = x] \\ =&F_i(U(x) - \frac{1}{3}\sin(x)) - F_i(L(x) - \frac{1}{3}\sin(x))\end{aligned}$$

where $F_i$ is the cumulative distribution function of $N(0, 0.1^2)$ for $i = 1$, $N(0, (0.1x)^2)$ for $i = 2$, and $0.1|x| \times t_4$ for $i = 3$. As shown in Figure 2 (b,c), the ground-truth conditional coverages of high-quality PIs diverge among different points, and they deviate from the marginal coverage. Thus, having access to the marginal coverage for the whole dataset is not sufficient for decision making, which highlights the need for conditional coverage. In addition, the conditional coverage estimator from our model is highly consistent with the conditional coverage on all of the synthetic examples in Figure 2. These results confirm that our CaNet can accurately estimate the conditional coverage on noisy datasets.

## 5.2 Performance of PIs on Benchmark Datasets

In this section, we compare the performance of PIs generated by the predictor module of our CaNet on real-world benchmark datasets with following baseline algorithms: (1) nearest-neighbors kernel conditional density estimation (NNKCDE) (Dalmasso et al. , 2020), (2) quantile regression forest (QRF) (Meinshausen , 2006), (3) split conformal learning (SCL) (Lei et al. , 2018) and (4) the quality-driven PI method (QD-Ens) (Pearce et al. , 2018). We quote the results from Pearce et al. (2018) as a comparison since we share the same experiment setup. Table 1 reports the results of $CP$, $IW$ and $ECE_1$ for generating PIs at 95% prediction level on benchmark datasets. We employed the criteria in Pearce et al. (2018) to evaluate the performance of PIs: the best $IW$ is achieved by the model with the smallest $IW$ value among those with $CP \geq 95\%$. As can be seen, our model achieves competitive results on PI generation under the high-quality criteria. With special consideration on interval width quality, it obtains the smallest average interval width ($IW$) while maintaining high coverage probability ($CP \geq 95\%$) on all datasets. These results show that adding an additional module CA-Module does not penalize the performance of PIs generated by our CaNet.

## 5.3 Performance of Coverage Estimator on Benchmark Datasets

**Coverage for 95% PIs.** We use $ECE_1$ to evaluate the coverage estimation performance on real-world datasets as the conditional coverage is unknown. As shown in Table 1, the $ECE_1$ on all experiments are generally around or less than 1%, with better performance on larger datasets. The coverage estimators produced by CaNet have small $ECE_1$ values, which are very close to the perfect-calibrated coverage estimators (Definition 2). Compared with $ECE_1$ values obtained from the state-of-the-art algorithms in classification tasks (Guo et al. , 2017; Kull , 2019), the $ECE_1$ values from CaNet are similar and sometimes less than their post-calibrated $ECE_1$ results (usually around 1% to 3%), even though the size of most regression datasets are smaller than the classification datasets. These results further demonstrate that our CaNet can accurately estimate the coverage information of 95% high-quality PIs on real-world regression tasks.

**Coverage for PIs at Different Prediction Levels.** We conduct multiple experiments on different PI prediction levels to show the robustness of our CaNet. By only modifying the parameter $\lambda_1$ in Equation 12, our Ca-Module could get access to different levels of coverage probability. Table 2 reports the $CP$, $IW$ and $ECE_1$ values from the CaNet at different PI pre-

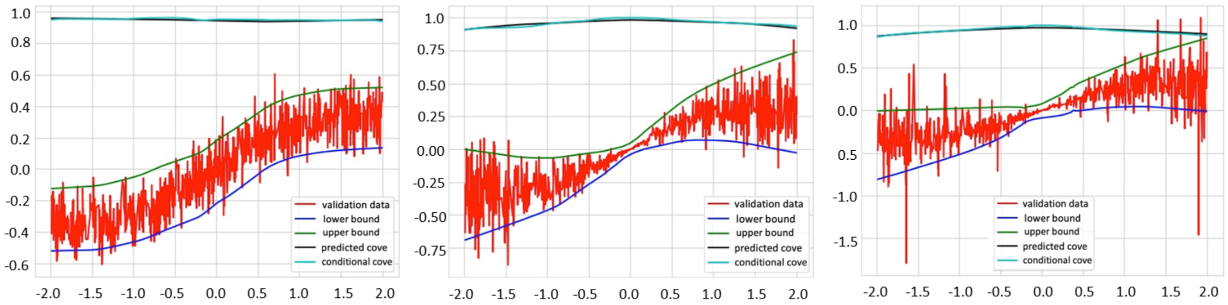

$(a)\ \varepsilon_1 \sim 0.1 \times N(0,1)$ $(b)\ \varepsilon_2 \sim 0.1|x| \times N(0,1)$ $(c)\ \varepsilon_3 \sim 0.1|x| \times t_4$

Figure 2: Prediction and conditional coverage of 95% PIs on synthetic examples. (a) $CP = 0.95$, $IW = 0.40$, $ECE_1 = 0.62\%$. (b) $CP = 0.96$, $IW = 0.40$, $ECE_1 = 0.12\%$. (c) $CP = 0.95$, $IW = 0.50$, $ECE_1 = 0.65\%$. The predicted coverage estimation from CaNet is highly consistent with the conditional coverage under different noise settings. The red curve represents the validation data. The dark blue curve represents the lower bound of the PI generated by our CaNet. The green curve represents the upper bound of the PI generated by our CaNet. The black curve represents the conditional coverage estimator generated by our CaNet. The light blue curve represents the ground-truth conditional coverage. In all figures, the conditional coverage estimator from our model (the black curve) is highly consistent with the ground-truth conditional coverage (the light blue curve). In Figure 2 (b,c), the ground-truth conditional coverages (the light blue curve) diverge among different points, highlighting the need for conditional coverage.

diction levels on three benchmark datasets. Results for more datasets can be found in Appendix D. As can be seen, all $ECE_1$ values in Table 2 are fairly small ($\sim 1\%$), demonstrating the stability of our proposed model. Thus, our CaNet can provide accurate coverage estimation on PIs at different prediction levels. These results demonstrate the robustness of our CaNet on real-world datasets, further suggesting its broad applicability.

# 6 Related Work

Finally, we discuss the connections of our paper with several lines of related work.

## 6.1 Prediction Interval Estimation

High-quality PIs, which can be viewed via a constrained optimization problem where the constraint concerns marginal coverage and the objective is the PI width, has been extensively studied in Khosravi et al. (2010, 2011); Galván et al. (2017); Pearce et al. (2018); Rosenfeld et al. (2018); Zhu et al. (2019); Chen et al. (2021). Such intervals are in the same spirit as the highest density intervals in statistics (Box and Tiao , 2011). While powerful, these approaches could not directly provide the conditional coverage information investigated in this work. Coverage-only criteria, on the other hand, focus solely on coverage satisfaction as the

| Dataset | NNKCDE |  | QRF |  | SCL |  | QD-Ens |  | CaNet: $\lambda_2 = 0.1^5$ for all datasets |  |  |  |  |
|---|---|---|---|---|---|---|---|---|---|---|---|---|---|
|  | $CP$ | $IW$ | $CP$ | $IW$ | $CP$ | $IW$ | $CP$ | $IW$ | $CP$ | $IW$ | $ECE_1$ | $\lambda_1$ | $\lambda_3$ |
| Boston | 0.95 | 1.54 | 0.96 | 2.22 | 0.97 | 1.45 | 0.92 | 1.16 | 0.95 | **1.04** | 1.38% | 6.0 | 1800 |
| Concrete | 0.95 | 1.85 | 0.99 | 2.53 | 0.96 | 1.54 | 0.94 | 1.09 | 0.95 | **1.13** | 0.24% | 6.5 | 1000 |
| Energy | 0.97 | 0.54 | 0.98 | 0.87 | 0.95 | 0.77 | 0.97 | 0.47 | 0.99 | **0.37** | 0.76% | 5.0 | 500 |
| Kin8nm | 0.99 | 2.76 | 0.99 | 3.27 | 0.94 | 1.20 | 0.96 | 1.25 | 0.95 | **1.04** | 1.32% | 3.6 | 300 |
| Plant | 0.95 | 0.88 | 0.97 | 1.05 | 0.95 | 0.88 | 0.95 | 0.86 | 0.95 | **0.84** | 0.38% | 3.3 | 700 |
| Protein | 0.93 | 1.98 | 0.98 | 2.42 | 0.95 | 2.81 | 0.95 | 2.27 | 0.95 | **2.26** | 0.41% | 8.3 | 300 |
| Wine | 0.96 | 2.64 | 0.93 | 3.18 | 0.96 | 3.44 | 0.92 | 2.33 | 0.95 | **2.59** | 0.42% | 19 | 1100 |
| Yacht | 0.95 | 1.15 | 0.95 | 1.72 | 0.95 | 0.57 | 0.96 | 0.17 | 0.98 | **0.16** | 0.80% | 1.6 | 500 |

Table 1: Evaluation metrics of different models on benchmark datasets. The $CP$ values are marked in blue if they meet the 95% prediction level. The best IW results, marked in bold, are achieved by models with the smallest IW value among those that meet the 95% prediction level. Our model outperforms the baseline algorithms on high-quality PI generation. Meanwhile, it provides accurate coverage estimation on real-world datasets.

guarantee. These approaches include conformal learning (CL) and its conditional variants (Vovk et al. , 2005, 2009; Lei and Wasserman , 2014; Lei et al. , 2015, 2018; Kuchibhotla and Ramdas , 2019; Romano et al. , 2019; Barber et al. , 2019a,b). CL is desirably distribution- or model-free, and in some cases enjoys finite-sample guarantees on coverage. However, the coverage guarantees from CL are only marginal with respect to the training data (except split CL (Vovk , 2012)). Moreover, unlike high-quality PIs, they do not explicitly account for the interval width as a quality metric. Nevertheless, we note that even in some literature with coverage-only consideration, interval width has also been implicitly served as a conservative measurement of PIs, e.g., in Zhang et al. (2019); Barber et al. (2019b). We also mention conditional density estimation (Holmes et al. , 2007; Dutordoir et al. , 2018; Izbicki and Lee , 2016; Dalmasso et al. , 2020; Freeman et al. , 2017; Izbicki et al. , 2017) and closely relatedly quantile regression (Koenker and Hallock , 2001; Meinshausen , 2006) as PI construction approaches by converting from the estimated conditional quantile function. These approaches focus on the quality of conditional distribution/quantile, instead of the high-quality criterion only. In this work, we follow some recent work using deep learning to achieve state-of-the-art performance for high-quality PIs construction (Khosravi et al. , 2010; Pearce et al. , 2018; Kivaranovic et al. , 2020).

## 6.2 Uncertainty Measurement in Deep Learning

Standard Bayesian approaches, e.g., Bayesian linear regression (Bishop , 2006), can be applied to construct PIs based on the posterior predictive distribution. But they usually assume that data follow a certain set of parameterized distributions, which provide a different perspective from the distribution-free, frequentist view taken in this paper. On the other hand, as for NNs, the Bayesian framework also offers a

| Kin8nm: $\lambda_2 = 0.1^5$, $\lambda_3 = 300$ | | | | Plant: $\lambda_2 = 0.1^5$, $\lambda_3 = 700$ | | | | Protein: $\lambda_2 = 0.1^5$, $\lambda_3 = 300$ | | | |
|---|---|---|---|---|---|---|---|---|---|---|---|
| $\lambda_1$ | $CP$ | $IW$ | $ECE_1$ | $\lambda_1$ | $CP$ | $IW$ | $ECE_1$ | $\lambda_1$ | $CP$ | $IW$ | $ECE_1$ |
| 1.9 | 0.83 | 0.73 | 1.54% | 1.4 | 0.80 | 0.56 | 1.23% | 4.8 | 0.82 | 1.56 | 0.82% |
| 2.1 | 0.85 | 0.77 | 1.59% | 1.5 | 0.84 | 0.62 | 1.36% | 5.1 | 0.86 | 1.70 | 0.71% |
| 2.3 | 0.87 | 0.80 | 1.47% | 1.6 | 0.85 | 0.63 | 0.86% | 5.4 | 0.88 | 1.79 | 1.25% |
| 2.4 | 0.88 | 0.84 | 1.21% | 1.8 | 0.86 | 0.64 | 1.36% | 5.6 | 0.90 | 1.84 | 1.04% |
| 2.6 | 0.90 | 0.87 | 1.50% | 2.0 | 0.89 | 0.70 | 0.51% | 6.3 | 0.91 | 1.95 | 0.66% |
| 2.9 | 0.91 | 0.89 | 0.50% | 2.4 | 0.91 | 0.75 | 1.15% | 6.5 | 0.92 | 2.07 | 1.36% |
| 3.1 | 0.92 | 0.94 | 0.49% | 2.6 | 0.92 | 0.80 | 1.29% | 7.0 | 0.93 | 2.11 | 1.23% |
| 3.4 | 0.94 | 1.00 | 0.82% | 3.0 | 0.94 | 0.83 | 0.23% | 7.8 | 0.94 | 2.13 | 0.99% |
| 3.6 | 0.95 | 1.04 | 1.32% | 3.3 | 0.95 | 0.84 | 0.38% | 8.3 | 0.95 | 2.26 | 0.41% |
| 3.8 | 0.96 | 1.06 | 1.25% | 4.0 | 0.96 | 0.89 | 0.80% | 9.3 | 0.96 | 2.36 | 0.52% |

Table 2: $ECE_1$ results of our model on benchmark datasets with different coverage probabilities. Our CaNet achieves robust performance on real-world datasets at different prediction levels.

principled approach for model uncertainty measurement by computing the posterior distribution over the NN parameters (MacKay , 1992; Neal , 2012). They focus on the parameter uncertainty of the NN instead of the coverage over a test point. In addition, exact Bayesian inference for deep Bayesian NNs is computationally intractable, making it less practical to implement. Gal and Ghahramani (2016) applied a Monte Carlo dropout method to proxy the inference. Directly generated from non-Bayesian networks, softmax response is also commonly used for uncertainty measurement on deep learning models (Bridle , 1990; Lakshminarayanan , 2017; Geifman et al. , 2018; Sensoy et al. , 2018; Ozbulak et al. , 2018). Moreover, Niculescu-Mizil and Caruana (2005) showed that NNs typically produce well-calibrated probabilities on binary classification tasks without the need for any post-hoc techniques. In this paper, we also follow this line of work and use the softmax output to access the model uncertainty information.

## 6.3 Simulation Metamodeling

Stochastic simulation aims to estimate a response surface of simulation outputs from complex stochastic models Barton and Meckesheimer (2006); Staum (2009). A common and versatile approach in simulation metamodeling is stochastic kriging (SK) Ankenman et al. (2008, 2010) which can handle general nonlinear input-output relations, and is also closely related to Gaussian process methodologies in Bayesian optimization Frazier (2018); Couckuyt et al. (2022). SK typically focuses on mean response surface estimation or quantile-based response measures Chen and Kim (2013); Bekki et al. (2014); Chen and Kim (2016), and can account for both epistemic and aleatory uncertainties, and as such allows to build PIs for the simulation random outputs. In addition to SK, recent work Lam and Zhang (2021, 2022) proposes to build PIs for simulation metamodeling by adapting techniques from machine learning including using the high-quality criterion and NNs, which is the approach considered in this paper. These studies mainly target at the marginal coverage of PIs while our methodology in this work aims to obtain conditional coverage information of PIs simultaneously.

## 7 Concluding Remarks

In this paper, we identify and investigate the conditional coverage estimation problem for high-quality PIs, which is critical for risk-based decision making in regression tasks including simulation metamodeling. To address the challenge, we propose an end-to-end algorithm with two powerful modules: the coverage assessment module and the predictor module. Benefiting from these powerful modules, our model can generate and validate the coverage estimator without any requirement for further post-processing steps. In addition, we conduct a theoretical analysis to show the effectiveness of our proposed model. Experimental results on synthetic examples and benchmark datasets further demonstrate that our model can robustly provide accurate coverage estimation while simultaneously producing a high-quality PI. Another alternative approach for conditional coverage estimation is a two-stage approach that considers the PI problem and the conditional coverage estimation problem separately in different networks. However, the two-stage approach is very complex and contains multiple steps that require two training processes for different networks. Essentially, we have to select more hyper-parameters for the two networks and also train more network weights to get the PI predictor and the conditional coverage estimator, which means more running time. Compared with the two-stage algorithm, our model has several advantages: our model is an end-to-end algorithm by leveraging the common feature layer (the last hidden layer) for both the PI predictor and the conditional coverage estimator, which is very concise and easy to implement. We can also efficiently choose the parameters via our tuning procedure. Moreover, our Ca-Module can be easily integrated into other deep-learning-based algorithms to access their conditional coverage information, opening up more opportunities for broad applications. In the future, we will extend our work by conducting comparison studies with Bayesian methods.

**Acknowledgement.** This work has been supported in part by the National Science Foundation under grants CAREER CMMI-1834710 and IIS-1849280. The research of Ziyi Huang and Haofeng Zhang is supported in part by the Cheung-Kong Innovation Doctoral Fellowship. The authors thank the reviewers and editors for their constructive comments which have helped greatly improve the quality of our paper.

## References

Ankenman B, Nelson B L, Staum J (2008). Stochastic kriging for simulation metamodeling. *Proceedings of the 2008 Winter Simulation Conference.* USA.

Ankenman B, Nelson B L, Staum J (2010). Stochastic kriging for simulation metamodeling. *Operations Research* 58(2): 371–382.

Anthony M, Bartlett P L (1999), *Neural Network Learning: Theoretical Foundations.* Cambridge university press, Cambridge.

Barber R F, Candes E J, Ramdas A, Tibshirani R J (2019a). The limits of distribution-free conditional predictive inference. *arXiv preprint arXiv:1903.04684.*

Barber R F, Candes E J, Ramdas A, Tibshirani R J (2019b). Predictive inference with the jackknife+. *arXiv preprint arXiv:1905.02928.*

Bartlett P L, Harvey N, Liaw C, Mehrabian A (2019). Nearly-tight VC-dimension and pseudodimension bounds for piecewise linear neural networks. *Journal of Machine Learning Research* 20(63): 1–17.

Barton R R, Meckesheimer M (2006). Metamodel-based simulation optimization. *Handbooks in operations research and manage- ment science.* North Holland, Netherlands.

Bekki J M, Chen X, Batur D (2014). Steady-state quantile parameter estimation: an empirical comparison of stochastic kriging and quantile regression. *Proceedings of the 2014 Winter Simulation Conference.* USA.

Bishop C M (2006). *Pattern recognition and machine learning.* Springer, USA.

Box G E, Tiao G C (2011). *Bayesian inference in statistical analysis.* John Wiley & Sons, USA.

Bridle J S (1990). Probabilistic interpretation of feedforward classification network outputs, with relationships to statistical pattern recognition. *Neurocomputing.* France.

Chen H, Huang Z, Lam H, Qian H, Zhang H (2021). Learning prediction intervals for regression: generalization and calibration. *International Conference on Artificial Intelli- gence and Statistics.* Virtual.

Chen X, Kim K-K (2013). Building metamodels for quantile-based measures using sectioning. *Proceedings of the 2013 Winter Simulation Conference.* USA.

Chen X, Kim K-K (2016). Efficient var and cvar measurement via stochastic kriging. *INFORMS Journal on Computing* 28(4): 629-644.

Couckuyt I, Gonzalez S R, Branke J (2022). Bayesian optimization: tutorial. *Proceedings of the Genetic and Evolutionary Computation Conference Companion.* USA.

Dalmasso N, Pospisil T, Lee A B, Izbicki R, Freeman P E, Malz A I (2020). Conditional density estimation tools in Python and R with applications to photometric redshifts and likelihood-free cosmological inference. *Astronomy and Computing* 30: 100362.

Dutordoir V, Salimbeni H, Hensman J, Deisenroth M (2018). Gaussian process conditional density estimation. *Advances in Neural Information Processing Systems.* Canada.

Fort S, Hu H, Lakshminarayanan B (2019). Deep ensembles: a loss landscape perspective. *arXiv preprint arXiv:1912.02757.*

Frazier P I (2018). A tutorial on Bayesian optimization. *arXiv preprint arXiv:1807.02811.*

Freeman P E, Izbicki R, Lee A B (2017). A unified framework for constructing, tuning and assessing photometric redshift density estimates in a selection bias setting. *Monthly No-*

*tices of the Royal Astronomical Society* 468 (4): 4556–4565.

Gal Y, Ghahramani Z (2016). Dropout as a Bayesian approximation: Representing model uncertainty in deep learning. *International Conference on Machine Learning.* USA.

Galván I M, Valls J M, Cervantes A, Aler R (2017). Multi-objective evolutionary optimization of prediction intervals for solar energy forecasting with neural networks. *Information Sciences* 418: 363–382.

Geifman Y, Uziel G, El-Yaniv R (2018). Bias-reduced uncertainty estimation for deep neural classifiers. *International Conference on Learning Representations.* Canada.

Guo C, Pleiss G, Sun Y, Weinberger K Q (2017). On calibration of modern neural networks. *International Conference on Machine Learning.* Australia.

Gustafsson F K, Danelljan M, Schon T B (2020). Evaluating scalable Bayesian deep learning methods for robust computer vision. *Proceedings of the IEEE/CVF Conference on Computer Vision and Pattern Recognition Workshops.* USA.

Hernández-Lobato J M, Adams R (2015). Probabilistic backpropagation for scalable learning of Bayesian neural networks. *International Conference on Machine Learning.* France.

Holmes M P, Gray A G, Isbell Jr C L (2007). Fast nonparametric conditional density estimation. *Uncertainty in Artificial Intelligence.* Canada.

Izbicki R, Lee A B (2016). Nonparametric conditional density estimation in a high-dimensional regression setting. *Journal of Computational and Graphical Statistics* 25(4): 1297–1316.

Izbicki R, Lee A B, Freeman P E (2017). Photo-z estimation: An example of nonparametric conditional density estimation under selection bias. *Annals of Applied Statistics* 11(2): 698-724.

Khosravi A, Nahavandi S, Creighton D, Atiya A F (2010). Lower upper bound estimation method for construction of neural network-based prediction intervals. *IEEE transactions on neural networks* 22(3): 337–346.

Khosravi A, Nahavandi S, Creighton D, Atiya A F (2011). Comprehensive review of neural network-based prediction intervals and new advances. *IEEE transactions on neural networks* 22(9): 1341–1356.

Kivaranovic D, Johnson K D, Leeb H (2020). Adaptive, distribution-free prediction intervals for deep networks. *International Conference on Artificial Intelligence and Statistics.* Italy.

Koenker R, Hallock K F (2001). Quantile regression. *Journal of economic perspectives* 15(4): 143–156.

Kosorok M R (2007). *Introduction to empirical processes and semiparametric inference.* Springer, USA.

Kuchibhotla A K, Ramdas A K (2019). Nested conformal prediction and the generalized jackknife+. *arXiv preprint arXiv:1910.10562.*

Kull M, Nieto M P, Kängsepp M, Silva Filho T, Song H, Flach P (2019) Beyond temperature scaling: Obtaining well-calibrated multiclass probabilities with Dirichlet calibration. *Advances in Neural Information Processing Systems.* Canada.

Kumar A, Liang P S, Ma T (2019). Verified uncertainty calibration. *Advances in Neural Information Processing Systems.* Canada.

Lakshminarayanan B, Pritzel A, Blundell C (2017). Simple and scalable predictive uncertainty estimation using deep ensembles. *Advances in Neural Information Processing Systems.* USA.

Lam H, Zhang H (2021). Neural predictive intervals for simulation metamodeling. *Proceedings of the 2021 Winter Simulation Conference.* USA.

Lam H, Zhang H (2022). Prediction intervals for simulation metamodeling. *arXiv preprint arXiv:2204.01904.*

Lee S, Purushwalkam S, Cogswell M, Crandall D, Batra D (2015). Why m heads are better than one: Training a diverse ensemble of deep networks. *arXiv preprint arXiv:1511.06314.*

Lei J, G'Sell M, Rinaldo A, Tibshirani R J, Wasserman L (2018). Distribution-free predictive inference for regression. *Journal of the American Statistical Association* 113(523): 1094–1111.

Lei J, Rinaldo A, Wasserman L (2015). A conformal prediction approach to explore functional data. *Annals of Mathematics and Artificial Intelligence* 74(1-2): 29–43.

Lei J, Wasserman L (2014). Distribution-free prediction bands for non-parametric regression. *Journal of the Royal Statistical Society: Series B (Statistical Methodology)* 76(1): 71–96.

MacKay D J (1992). Bayesian methods for adaptive models. *Ph.D. thesis, California Institute of Technology.*

Massart P (2007). *Concentration inequalities and model selection.* Springer, USA.

Meinshausen N (2006). Quantile regression forests. *Journal of Machine Learning Research* 7: 983–999.

Neal R M (2012). *Bayesian learning for neural networks.* Springer, USA.

Niculescu-Mizil A, Caruana R (2005). Predicting good probabilities with supervised learning. *International Conference on Machine Learning.* Germany.

Nixon J, Dusenberry M, Zhang L, Jerfel G, Tran D (2019). Measuring calibration in deep learning. *arXiv preprint arXiv:1904.01685.*

Ovadia Y, Fertig E, Ren J, Nado Z, Sculley D, Nowozin S, Dillon J, Lakshminarayanan B, Snoek J (2019). Can you trust your model's uncertainty? evaluating predictive uncertainty under dataset shift. *Advances in Neural Information Processing Systems.* Canada.

Ozbulak U, De Neve W, Van Messem A (2018). How the softmax output is misleading for evaluating the strength of adversarial examples. *arXiv preprint arXiv:1811.08577.*

Pearce T, Leibfried F, Brintrup A (2020). Uncertainty in neural networks: Approximately Bayesian ensembling. *International conference on artificial intelligence and statistics.* Virtual.

Pearce T, Zaki M, Brintrup A, Neely A (2018). High-quality prediction intervals for deep learning: A distribution-free, ensembled approach. *arXiv preprint arXiv:1802.07167.*

Romano Y, Patterson E, Candes E (2019). Conformalized quantile regression. *Advances in Neural Information Processing Systems.* Canada.

Rosenfeld N, Mansour Y, Yom-Tov E (2018). Discriminative learning of prediction intervals. *International Conference on Artificial Intelligence and Statistics.* Spain.

Sensoy M, Kaplan L, Kandemir M (2018). Evidential deep learning to quantify classification uncertainty. *Advances in Neural Information Processing Systems.* Canada.

Sontag E D (1998). VC dimension of neural networks. *NATO ASI Series F Computer and Systems Sciences* 168: 69–96.

Staum J (2009). Better simulation metamodeling: The why, what, and how of stochastic kriging. *Proceedings of the 2009 Winter Simulation Conference.* USA.

Tagasovska N, Lopez-Paz D (2018). Frequentist uncertainty estimates for deep learning. *arXiv preprint arXiv:1811.00908.*

Tagasovska N, Lopez-Paz D (2019). Single-model uncertainties for deep learning. *Advances in Neural Information Processing Systems.* Canada.

Van der Vaart A W, Wellner J A (1996). *Weak Convergence and Empirical Processes with Applications to Statistics.* Springer. USA.

Vovk V (2012). Conditional validity of inductive conformal predictors. *Asian conference on machine learning.* Singapore.

Vovk V, Gammerman A, Shafer G (2005). *Algorithmic learning in a random world.* Springer. USA.

Vovk V, Nouretdinov I, Gammerman A (2009). On-line predictive linear regression. *The Annals of Statistics* 37(3): 1566–1590.

Wang B, Lu J, Yan Z, Luo H, Li T, Zheng Y, Zhang G (2019). Deep uncertainty quantification: A machine learning approach for weather forecasting. *Proceedings of the 25th ACM SIGKDD International Conference on Knowledge Discovery and Data Mining.* USA.

Zhang H, Zimmerman J, Nettleton D, Nordman D J (2019). Random forest prediction intervals. *The American Statistician* 74(4): 392-406.

Zhu L, Lu J, Chen Y (2019). HDI-forest: highest density interval regression forest. *Proceedings of the 28th International Joint Conference on Artificial Intelligence.* China.

**Ziyi Huang** is a Ph.D. student in the Department of Electrical Engineering at Columbia University, New York, USA. Her research aims to develop deep learning algorithms for better image intervention and address data quality challenges for real-world applications. Her email address is zh2354@columbia.edu.

**Henry Lam** is an Associate Professor in the Department of Industrial Engineering and Operations Research at Columbia University. His research interests include Monte Carlo methods, uncertainty quantification, data-driven optimization and rare-event analysis. His works have been recognized by several venues such as the NSF CAREER Award, JP Morgan Chase Faculty Research Award and Adobe Faculty Research Award. Henry serves on the editorial boards of *Operations Research*, *INFORMS Journal on Computing*, *Applied Probability Journals*, *Stochastic Models*, *Manufacturing and Service Operations Management*, and *Queueing Systems*, and as the Area Editor in Stochastic Models and Data Science in *Operations Research Letters*. Henry received his PhD degree in statistics from Harvard University. His email address is henry.lam@columbia.edu.

**Haofeng Zhang** is a Ph.D. student in the Department of Industrial Engineering and Operations Research at Columbia University, New York, USA. His primary research interests lie in applying Monte Carlo simulation, uncertainty quantification, and stochastic optimization to developing data-driven predictive and decision-making methodologies. His email address is hz2553@columbia.edu.

# Appendices

This appendix presents further results and discussions and it consists of four parts. Appendix A gives more detailed properties on coverage estimator and coverage error. Appendix B contains the mathematical argument for Theorem 1. Appendix C discusses how to achieve Assumption 1 and the proof of Theorem 2 and 3. Appendix D illustrates experimental details and more experimental results.

## A Further Details on Coverage Estimator and Coverage Error

### A.1 Coverage Probability Types of PIs

Zhang et al. (2019) introduce the following four coverage probability types of PIs. In general, most of the coverage in PIs considered in the literature falls into one of these types.

Type I: $\mathbb{P}[Y \in [L(X), U(X)]]$ (marginal coverage);

Type II: $\mathbb{P}[Y \in [L(X), U(X)]|L, U]$ (conditional coverage given the PI);

Type III: $\mathbb{P}[Y \in [L(X), U(X)]|X = x]$ (conditional coverage given $X = x$);

Type IV: $\mathbb{P}[Y \in [L(X), U(X)]|L, U, X = x]$ (conditional coverage given the PI and $X = x$).

Note that in high-quality criteria, only Type II coverage is considered in the constraint but Type IV coverage is lacking. Since Type I and III are not considered in our paper, for simplicity Type II coverage is called the marginal coverage, and Type IV coverage is called the conditional coverage in Definition 1.

Throughout Appendix, we let $A(x) := \mathbb{P}[Y \in [L(X), U(X)]|L, U, X = x]$ denote the conditional coverage in Definition 1. Moreover, since we only concern Type II and IV coverage in this work, we make the following convention. Throughout Appendix A-B, $\mathbb{P}$ and $\mathbb{E}$ should be understood as probability and expectation conditional on $L, U$. So for $A(x)$, we could simply write $A(x) := \mathbb{P}[Y \in [L(X), U(X)]|X = x]$ and omit "conditional on $L, U$".

### A.2 The Terminology "Perfect-Calibrated"

The terminology "perfect-calibrated" is borrowed from the confidence calibration in classification tasks. We first review the name of "confidence" in classification.

Confidence calibration is the problem of predicting probability estimates representative of the true correctness likelihood (Guo et al. , 2017). Intuitively, an reliable confidence should reflect the true correctness likelihood of the prediction (Kumar , 2019). For example, given 100 predictions, each with confidence of 0.8, we expect that 80 should be correctly classified (Guo et al. , 2017).

Now let $h$ be the prediction of any models, which is a map from $\mathcal{X}$ to $\mathcal{Y}$, trained on the data

$\mathcal{D}$. According to their definition, the "best" confidence map $\hat{P}$ should be the true probability of correctness:

$$\hat{P}(x) = \mathbb{E}[\mathbf{1}_{h(X) \text{ is correct for } Y}|h, X = x], \quad \forall x \in \mathcal{X}. \tag{14}$$

which is a measureable function from $\mathcal{X}$ to $[0, 1]$. In particular, we consider $h$ as a PI in regression tasks and "correctness" of a PI is naturally defined as the success of coverage on the outcome $Y$. Then the right hand side of Equation (14) becomes

$$\begin{aligned}\mathbb{E}[\mathbf{1}_{h(X) \text{ is correct for } Y}|h, X = x] &= \mathbb{E}[\mathbf{1}_{Y\in[L(X),U(X)]}|L, U, X = x] \\ &= \mathbb{P}[Y \in [L(X), U(X)]|L, U, X = x].\end{aligned}$$

which is the conditional coverage in our Definition 1.

In addition, Guo et al. (2017) introduce the perfect-calibrated confidence as follows:

$$\mathbb{P}(\hat{Y} = Y|\hat{Y}, \hat{P} = p) = p, \quad \forall p \in [0, 1]$$

where $\hat{Y}$ is the class prediction and $\hat{Y} = Y$ means that the predicted and true class label coincide. Obviously, if $\hat{P}(X) = \mathbb{P}(\hat{Y}(X) = Y|X)$, i.e., the "best" confidence, then the above equality holds. Transferring this idea into PIs, we can naturally define the perfect-calibrated coverage estimator as

$$p = \mathbb{E}[\mathbf{1}_{h(X) \text{ is correct for } Y}|L, U, \hat{P} = p] = \mathbb{P}[Y \in [L(X), U(X)]|L, U, \hat{P} = p], \quad \forall p \in [0, 1].$$

which is the conditional coverage in our Definition 2.

### A.3 Details on Coverage Estimator

A perfect-calibrated coverage estimator inherits some properties of a conditional coverage. For example, both of them have the following interpretation: If we have 1000 testing points for a PI, each with the same conditional/perfect-calibrated coverage 0.9, then approximately 900 of them are correctly covered by the PI. Note that the conditional coverage is uniquely defined, but a perfect-calibrated coverage estimator is not necessarily so. Moreover, we have the following facts: (a) The conditional coverage is always perfect-calibrated, but not vice versa. (b) A perfect-calibrated coverage estimator can be viewed as an averaged conditional coverage. (c) A perfect-calibrated coverage estimator is less "informative" than the conditional coverage.

**A perfect-calibrated coverage estimator is an averaged conditional coverage.** Let $\hat{P}$

be a (general) coverage estimator. We have

$$\begin{aligned}
&\mathbb{P}[Y \in [L(X), U(X)] | \hat{P}(X) = \hat{P}(x)] \\
=&\mathbb{P}[Y \in [L(X), U(X)] | X \in \hat{P}^{-1}(\hat{P}(x))] \\
=&\frac{\mathbb{P}[Y \in [L(X), U(X)], X \in \hat{P}^{-1}(\hat{P}(x))]}{\mathbb{P}[X \in \hat{P}^{-1}(\hat{P}(x))]} \\
=&\frac{\int_{t \in \hat{P}^{-1}(\hat{P}(x))} \mathbb{E}[\mathbf{1}_{Y \in [L(X), U(X)]} | X = t] \mathbb{P}[X \in dt]}{\mathbb{P}[X \in \hat{P}^{-1}(\hat{P}(x))]} \\
=&\frac{\int_{t \in \hat{P}^{-1}(\hat{P}(x))} A(t) \mathbb{P}[X \in dt]}{\mathbb{P}[X \in \hat{P}^{-1}(\hat{P}(x))]}
\end{aligned}$$

Suppose $\hat{P}$ is a perfect-calibrated coverage estimator. Then we have

$$\hat{P}(x) = \frac{\int_{t \in \hat{P}^{-1}(\hat{P}(x))} A(t) \mathbb{P}[X \in dt]}{\mathbb{P}[X \in \hat{P}^{-1}(\hat{P}(x))]}$$

which implies that $\hat{P}(x)$ is a weighted average of $A(t)$ over the set $\hat{P}^{-1}(\hat{P}(x))$ with weights based on the marginal distribution of $X$.

**A conditional coverage is perfect-calibrated.** If $\hat{P}(x) = A(x)$, then $A(t) = A(x)$ for any $t \in A^{-1}(A(x))$ so

$$\frac{\int_{t \in A^{-1}(A(x))} A(t) \mathbb{P}[X \in dt]}{\mathbb{P}[X \in A^{-1}(A(x))]} = \frac{A(x) \int_{t \in A^{-1}(A(x))} \mathbb{P}[X \in dt]}{\mathbb{P}[X \in A^{-1}(A(x))]} = A(x).$$

This shows that $A(x)$ must be a perfect-calibrated coverage estimator. Another way to see this is taking conditional expectation given $A(X) = p$ in the Definition 1. Then we get

$$\begin{aligned}
p &= \mathbb{E}[A(X) | A(X) = p] \\
&= \mathbb{E}[\mathbb{P}[Y \in [L(X), U(X)] | X] | A(X) = p] \\
&= \mathbb{P}[Y \in [L(X), U(X)] | A(X) = p] \quad \text{by the tower property.}
\end{aligned}$$

**A perfect-calibrated coverage estimator may be less informative and may not be the conditional coverage.** Suppose we have a PI $[L(X), U(X)]$ at the exact prediction level of $1 - \alpha$, i.e., $\mathbb{P}[Y \in [L(X), U(X)]] = 1 - \alpha$. Then the constant coverage estimator

$$\hat{P}(x) = 1 - \alpha, \quad \forall x \in \mathcal{X}$$

can be viewed as an average coverage estimator over the entire space $\mathcal{X}$. It is a perfect-calibrated coverage estimator since by definition,

$$\mathbb{P}[Y \in [L(X), U(X)] | \hat{P}(X) = 1 - \alpha] = \mathbb{P}[Y \in [L(X), U(X)]] = 1 - \alpha = \hat{P}(X).$$

But it is not a conditional coverage in general (e.g., the second/third synthetic example in Section 5.1).

In the main paper, we have given the following extension of the definition of "perfect-calibrated" coverage estimator, allowing it to be defined on any positive-probability measurable subsets.

**Definition 6** (Restated Definition 5)**.** *A coverage estimator $\hat{P}$ is called a perfect-calibrated coverage estimator on a measurable subset $\mathcal{S} \subset \mathcal{X}$ with $\mathbb{P}(\mathcal{S}) > 0$ associated with $[L(x), U(x)]$ if it satisfies*

$$\hat{P}(x) = \mathbb{P}[Y \in [L(X), U(X)] | L, U, \hat{P}(X) = \hat{P}(x), X \in \mathcal{S}], \quad a.e.\ \hat{P}(x) \in [0, 1]. \tag{15}$$

*where a.e. is with respect to the probability measure on $[0, 1]$ induced by the random variable $\hat{P}(X|_{\mathcal{S}})$. Note that the conditional probability space is standard: $(\mathcal{S}, \mathcal{F}_{\mathcal{S}} := \{A \cap \mathcal{S} : A \in \mathcal{F}\}, \mathbb{P}_{\mathcal{S}}(A \cap \mathcal{S}) := \mathbb{P}(A|\mathcal{S}))$.*

(As our convention in Section A.1, we will omit "conditional on $L, U$" for simplicity.)

**Lemma 2** (Restated Lemma 1)**.** *(a) A coverage estimator is the conditional coverage if and only if it is a perfect-calibrated coverage estimator on any positive-probability measurable subset $\mathcal{S}$ of $\mathcal{X}$. (b) Suppose $\hat{P}$ is a perfect-calibrated coverage estimator on two disjoint positive-probability measurable subsets $\mathcal{S}_1$, $\mathcal{S}_2$. Then $\hat{P}$ is a perfect-calibrated coverage estimator on $\mathcal{S}_1 \cup \mathcal{S}_2$.*

*Proof.* (a) The proof can be found in Lemma 3.

(b) We note that by law of total probability,

$$\begin{aligned}
&\mathbb{P}[Y \in [L(X), U(X)] | \hat{P}(X) = p, X \in \mathcal{S}_1 \cup \mathcal{S}_2] \\
=&\mathbb{P}[Y \in [L(X), U(X)] | \hat{P}(X) = p, X \in \mathcal{S}_1] \mathbb{P}[X \in \mathcal{S}_1 | \hat{P}(X) = p, X \in \mathcal{S}_1 \cup \mathcal{S}_2] \\
&+ \mathbb{P}[Y \in [L(X), U(X)] | \hat{P}(X) = p, X \in \mathcal{S}_2] \mathbb{P}[X \in \mathcal{S}_2 | \hat{P}(X) = p, X \in \mathcal{S}_1 \cup \mathcal{S}_2] \\
=&p(\mathbb{P}[X \in \mathcal{S}_1 | \hat{P}(X) = p, X \in \mathcal{S}_1 \cup \mathcal{S}_2] + \mathbb{P}[X \in \mathcal{S}_2 | \hat{P}(X) = p, X \in \mathcal{S}_1 \cup \mathcal{S}_2]) \\
=&p.
\end{aligned}$$

Hence $\hat{P}$ is a perfect-calibrated coverage estimator on $\mathcal{S}_1 \cup \mathcal{S}_2$. □

Lemma 1(a) is motivated from a theoretical point of view. It provides a guidance that in order to well resemble the conditional coverage, an estimator should be perfect-calibrated on as many subsets on the feature space as possible.

### A.4 Details on Coverage Error

In Section 2, we have introduced $CE_p$ to quantify the discrepancy between a coverage estimator and a perfect-calibrated coverage estimator, and $\widetilde{CE}_p$ to quantify the discrepancy between a coverage estimator and the conditional coverage. We note that by Hölder's inequality

$$CE_p \leq CE_q, \text{ for } 1 \leq p \leq q \leq +\infty.$$

A larger value of $p$ corresponds to a larger $CE$ value. Continuing Definition 5, we can further introduce the calibration-based conditional coverage error on a measurable subset as follows:

**Definition 7.** *An $L^p$ ($1 \le p \le +\infty$) calibration-based conditional coverage error, or coverage error for short, of a coverage estimator $\hat{P}$ on a measurable subset $\mathcal{S} \subset \mathcal{X}$ with $\mathbb{P}(\mathcal{S}) > 0$ is defined as:*

$$CE_p(\mathcal{S}) = \left\| \mathbb{P}[Y \in [L(X), U(X)] | L, U, \hat{P}(X), X \in \mathcal{S}] - \hat{P}(X) \right\|_{L^p(\mathcal{S})} \tag{16}$$

*where $L^p$-norm is taken with respect to the randomness of $\hat{P}(X)$ on the conditional probability space $(\mathcal{S}, \mathcal{F}_{\mathcal{S}} := \{A \cap \mathcal{S} : A \in \mathcal{F}\}, \mathbb{P}_{\mathcal{S}}(A \cap \mathcal{S}) := \mathbb{P}(A|\mathcal{S}))$. In particular, we have $CE_p := CE_p(\mathcal{X})$.*

**Lemma 3.** *A coverage estimator $\hat{P}$ is the conditional coverage if and only if its coverage error $CE_p(\mathcal{S}) = 0$ for any measurable subset $\mathcal{S} \subset \mathcal{X}$ with $\mathbb{P}(\mathcal{S}) > 0$. In particular, a coverage estimator is the conditional coverage if and only if it is a perfect-calibrated coverage estimator on any measurable subset $\mathcal{S}$ of $\mathcal{X}$ with $\mathbb{P}(\mathcal{S}) > 0$.*

*Proof.* We first show that the conditional coverage is perfect-calibrated. Taking conditional expectation given $\{A(X) = p, X \in \mathcal{S}\}$ in the Definition 1. Then we get

$$\begin{aligned} p &= \mathbb{E}[A(X) | A(X) = p, X \in \mathcal{S}] \\ &= \mathbb{E}[\mathbb{P}[Y \in [L(X), U(X)] | X] | A(X) = p, X \in \mathcal{S}] \\ &= \mathbb{P}[Y \in [L(X), U(X)] | A(X) = p, X \in \mathcal{S}] \quad \text{by the tower property.} \end{aligned}$$

So $A(x)$ is a perfect-calibrated coverage estimator on any measurable subset $\mathcal{S}$ with $\mathbb{P}(\mathcal{S}) > 0$. Hence $CE_p(\mathcal{S}) = 0$ for any measurable subsets $\mathcal{S} \subset \mathcal{X}$ with $\mathbb{P}(\mathcal{S}) > 0$.

On the other hand, similarly to Section A.3, we can express

$$\mathbb{P}[Y \in [L(X), U(X)] | \hat{P}(X) = \hat{P}(x), X \in \mathcal{S}] = \frac{\int_{t \in \hat{P}^{-1}(\hat{P}(x)) \cap \mathcal{S}} A(t) \mathbb{P}[X \in dt]}{\mathbb{P}[X \in \hat{P}^{-1}(\hat{P}(x)) \cap \mathcal{S}]}.$$

Suppose $\hat{P}(x)$ is not the conditional coverage, then $\mathbb{P}[\hat{P}(X) \neq A(X)] > 0$. Without loss of generality, we assume $\mathbb{P}[\hat{P}(X) > A(X)] > 0$. Let $\mathcal{S}_0 := \{x \in \mathcal{X} : \hat{P}(x) > A(x)\}$. Note that $\mathcal{S}_0 = \cup_{n=1}^{+\infty} \{x \in \mathcal{X} : \hat{P}(x) > A(x) + \frac{1}{n}\}$. Since $\mathbb{P}(\mathcal{S}_0) > 0$, there exists a $n_0$ such that $\mathcal{S} := \{x \in \mathcal{X} : \hat{P}(x) > A(x) + \frac{1}{n_0}\}$ and $\mathbb{P}(\mathcal{S}) > 0$.

Then for $x \in \mathcal{S}$, we have

$$\frac{\int_{t \in \hat{P}^{-1}(\hat{P}(x)) \cap \mathcal{S}} A(t) \mathbb{P}[X \in dt]}{\mathbb{P}[X \in \hat{P}^{-1}(\hat{P}(x)) \cap \mathcal{S}]} \le \frac{\int_{t \in \hat{P}^{-1}(\hat{P}(x)) \cap \mathcal{S}} (\hat{P}(t) - \frac{1}{n_0}) \mathbb{P}[X \in dt]}{\mathbb{P}[X \in \hat{P}^{-1}(\hat{P}(x)) \cap \mathcal{S}]} = \hat{P}(x) - \frac{1}{n_0}.$$

Then we have

$$CE_p(\mathcal{S}) \ge CE_1(\mathcal{S}) \ge \frac{1}{n_0} > 0$$

so $CE_p(\mathcal{S}) > 0$, which is a contradiction. Hence $\hat{P}(x)$ is the conditional coverage. □

# B Mathematical Developments for Theorem 1

This section proves Theorem 1: we show that both coverage error and conditional coverage error are tightly bounded above by the expectation of a Kullback–Leibler divergence-type random variable $K_1(x)$. This means that minimizing $\mathbb{E}[K_1(X)]$ can recover the true conditional coverage and effectively reduce the coverage error. The proof consists of several inequalities regarding coverage errors and their relations. We first begin with the following connection between $CE_p$ and $\widetilde{CE}_p$.

**Theorem 4.** *For any PI and its associated $\hat{P}$, the $L^p$ coverage error is always less than or equal to the $L^p$ conditional coverage error, i.e.,*

$$CE_p \leq \widetilde{CE}_p, \quad \forall 1 \leq p \leq +\infty$$

*Proof.* We note that the function $t \mapsto |t|^p$ is a convex function. We also note that $\sigma(\hat{P}(X)) \subset \sigma(X)$ where $\sigma(Y)$ represents the $\sigma$-field generated by a random variable $Y$.

$$\begin{aligned}
\widetilde{CE}_p^p =& \mathbb{E}\left[\left|A(X) - \hat{P}(X)\right|^p\right] \\
=& \mathbb{E}\left[\mathbb{E}|A(x) - \hat{P}(X)|^p|\hat{P}(X)]\right] \\
\geq& \mathbb{E}\left[\left|\mathbb{E}[A(x) - \hat{P}(X)|\hat{P}(X)]\right|^p\right] \quad \text{by Jensen's inequality} \\
=& \mathbb{E}\left[\left|\mathbb{E}[\mathbf{1}_{Y\in[L(X),U(X)]}|\hat{P}(X)] - \hat{P}(X)\right|^p\right] \quad \text{by the tower property} \\
=& CE_p^p
\end{aligned}$$

Therefore we have

$$CE_p \leq \widetilde{CE}_p, \quad \forall 1 \leq p \leq +\infty.$$

□

Next we have the following bounds on $L^p$ conditional coverage error:

**Theorem 5.** *The $L^p$ conditional coverage error is bounded above by a power function of the $L^2$ conditional coverage error. Formally,*

$$\widetilde{CE}_p \leq \widetilde{CE}_2^{\alpha_p}, \quad \forall 1 \leq p \leq +\infty,$$

*where $\alpha_p = 1, \forall 1 \leq p \leq 2$ and $\alpha_p = \frac{2}{p}, \forall 2 \leq p \leq +\infty$.*

*Proof.* By Hölder's inequality,

$$\widetilde{CE}_p \leq \widetilde{CE}_2, \text{ if } 1 \leq p \leq 2.$$

Since

$$0 \leq |A(x) - \hat{P}(x)| \leq 1,$$

then,

$$|A(x) - \hat{P}(x)|^p \leq |A(x) - \hat{P}(x)|^2, \quad \forall p \geq 2$$

and thus

$$\widetilde{CE}_p^p = \mathbb{E}[|A(X) - \hat{P}(X)|^p] \leq \mathbb{E}[|A(X) - \hat{P}(X)|^2] \leq \widetilde{CE}_2^2, \quad \forall p \geq 2.$$

□

Next, recall that

$$K(x) = A(x)\log\left(\frac{A(x)}{\hat{P}(x)}\right) + (1 - A(x))\log\left(\frac{1 - A(x)}{1 - \hat{P}(x)}\right),$$

$$K_0(x) = A(x)\log(A(x)) + (1 - A(x))\log(1 - A(x)),$$

$$K_1(x) = -A(x)\log(\hat{P}(x)) - (1 - A(x))\log(1 - \hat{P}(x)).$$

**Theorem 6.** *The $L^2$ conditional coverage error is bounded above by the expectation of $K(x)$. Formally,*

$$\widetilde{CE}_2^{\alpha_p} \leq \left(\frac{1}{2}\mathbb{E}[K(X)]\right)^{\alpha_p/2},$$

*where $\alpha_p$ is defined in Theorem 5.*

*Proof.* For any fixed $x$, consider two random variables with Bernoulli distributions:

$$W_1 = \begin{cases} 1 & \text{w.p. } A(x), \\ 0 & \text{w.p. } 1 - A(x). \end{cases}$$

$$W_2 = \begin{cases} 1 & \text{w.p. } \hat{P}(x), \\ 0 & \text{w.p. } 1 - \hat{P}(x). \end{cases}$$

Let $P_i$ be the distribution of $W_i$. It follows from Pinsker's inequality, e.g., Theorem 2.16 in (Massart , 2007), that

$$\|P_1 - P_2\|_{TV}^2 \leq \frac{1}{2}K(P_1, P_2).$$

where $TV$ denotes the total variation distance and $K$ denotes the KL divergence. Since $P_i$ is the Bernoulli distribution, we can express it as

$$|A(x) - P(x)|^2 \leq \frac{1}{2}K(x)$$

Taking expectation, we obtain

$$\mathbb{E}[|A(X) - P(X)|^2] \leq \frac{1}{2}\mathbb{E}[K(X)].$$

Hence,

$$\widetilde{CE}_2^{\alpha_p} \leq \left(\frac{1}{2}\mathbb{E}[K(X)]\right)^{\alpha_p/2}.$$

□

Combining Theorem 4, 5 and 6, we immediately conclude that:

**Theorem 7** (Restated Theorem 1)**.**

$$CE_p \leq \widetilde{CE}_p \leq \widetilde{CE}_2^{\alpha_p} \leq \left(\frac{1}{2}\mathbb{E}[K(X)]\right)^{\alpha_p/2}, \quad \forall 1 \leq p \leq +\infty$$

*where $\alpha_p$ is defined in Theorem 5. Moreover, all inequalities are attainable, e.g., if $\hat{P}(x)$ is the conditional coverage $A(x)$.*

# C Justification of Assumption 1 and Mathematical Developments for Theorem 3

In this section, we analyze the rationality of Assumption 1 and build essential ingredients for proving Theorem 2 and 3. The difficulty in analyzing Theorem 3 lies in the fact that the hypothesis classes in Assumption 1 (which are constructed by the NN) are different from the hypothesis class used in $L_{CA}$. To overcome this difficulty, we use the theory of VC-subgraph classes to analyze the connection between the VC dimension of the two hypothesis classes.

## C.1 Review of the VC Dimension

For self-contained purpose, we first review the definition of the VC-subgraph class and VC dimension.

**Definition 8.** *Consider an arbitrary collection $\{x_1, \cdots, x_n\}$ of points in a set $\mathcal{X}$ and a collection $\mathcal{C}$ of subsets of $\mathcal{X}$. We say that $\mathcal{C}$ shatters $\{x_1, \cdots, x_n\}$ if all of $2^n$ possible subsets of $\{x_1, \cdots, x_n\}$ can be written as $A = C \cap \{x_1, \cdots, x_n\}$ for some $C \in \mathcal{C}$. The VC dimension $V(\mathcal{C})$ of the class $\mathcal{C}$ is the smallest $n$ for which no set of size $n$ $\{x_1, \cdots, x_n\}$ is shattered by $\mathcal{C}$. If $\mathcal{C}$ shatters sets of arbitrarily large size, we set $V(\mathcal{C}) = \infty$. We say that $\mathcal{C}$ is a VC-class if $V(\mathcal{C}) < \infty$.*

In some literature, the VC dimension $V(\mathcal{C})$ of the class $\mathcal{C}$ is alternatively defined as the largest $n$ for which there exists a set of size $n$ $\{x_1, \cdots, x_n\}$ shattered by $\mathcal{C}$, i.e., it is the value in definition 8 minus 1. We can more formally define the VC dimension by the growth function as follows:

**Definition 9.** *Define the $n^{th}$ shatter coefficient (or growth function) of $\mathcal{C}$ as*

$$\Pi_{\mathcal{C}}(n) := \max_{x_1, \cdots, x_n} |\{A : A = C \cap \{x_1, \cdots, x_n\} \textit{ for some } C \in \mathcal{C}\}|$$

*Then*

$$V(\mathcal{C}) := \inf\{n : \Pi_{\mathcal{C}}(n) < 2^n\}.$$

**Definition 10.** *For a function $f : \mathcal{X} \to \mathbb{R}$, the subset of $\mathcal{X} \times \mathbb{R}$ given by $\{(x, t) : t < f(x)\}$ is the (open) subgraph of $f$. A collection $\mathcal{F}$ of measurable real functions on the sample space $\mathcal{X}$ is a VC-subgraph class or VC-class, if the collection of all subgraphs of functions in $\mathcal{F}$ forms a VC-class of sets (as sets in $\mathcal{X} \times \mathbb{R}$). Let $V(\mathcal{F})$ denote the VC dimension of the set of subgraphs of $\mathcal{F}$.*

**Lemma 4.** *In Definition 10, the open subgraph of $f$, $\{(x, t) : t < f(x)\}$, can be replaced by the close subgraph $\{(x, t) : t \leq f(x)\}$, the close supergraph $\{(x, t) : t \geq f(x)\}$ or the open supergraph $\{(x, t) : t > f(x)\}$. All of them lead to the equivalent definition of the VC-class and the equal VC dimension.*

*Proof.* This result follows from Lemma 9.33 and Lemma 9.9(iv) in Kosorok (2007). □

For indicator functions of sets, we have the following equivalence.

**Lemma 5.** *For any class $\mathcal{C}$ of sets in a set $\mathcal{X}$, the class $\mathcal{F}_{\mathcal{C}}$ of indicator functions of sets in $\mathcal{C}$ is a VC-class if and only if $\mathcal{C}$ is a VC-class. Moreover, whenever at least one of $\mathcal{C}$ or $\mathcal{F}_{\mathcal{C}}$ is VC-class, the respective VC dimensions are equal.*

*Proof.* This is Lemma 9.8 in Kosorok (2007). Note that the sets of $\mathcal{C}$ are in $\mathcal{X}$ while the subgraphs of functions of $\mathcal{F}_{\mathcal{C}}$ are in $\mathcal{X} \times \mathbb{R}$. □

### C.2 Justifying Assumption 1

We first restate the assumption:

**Assumption 3** (Restated Assumption 1)**.** *The four classes of functions $([L(x), U(x)], \hat{P}(x), 1 - \hat{P}(x))$ output by the neural network (NN) in Figure 1 have finite VC dimensions, say they are bounded above by $V_0$.*

In Figure 1, the output four neurons of the NN are denoted as $(L(x), U(x), \hat{P}(x), 1 - \hat{P}(x))$. We further let $(\psi_1(x), \psi_2(x), \psi_3(x), \psi_4(x))$ denote the pre-activated values of $(L(x), U(x), \hat{P}(x), 1 - \hat{P}(x))$. In other words,

$$L(x) = \min(\psi_1(x), \psi_2(x)),$$

$$U(x) = \max(\psi_1(x), \psi_2(x)),$$

$$\hat{P}(x) = \text{softmax}(\psi_3(x) || \psi_4(x)) = \sigma(\psi_3(x) - \psi_4(x)),$$

$$1 - \hat{P}(x) = \text{softmax}(\psi_4(x) || \psi_3(x)) = \sigma(\psi_4(x) - \psi_3(x)),$$

where $\sigma$ is the sigmoid function. Let the function classes

$$\mathcal{H}_1 = \{L(x) : L \text{ is output by the the NN}\},$$

$$\mathcal{H}_2 = \{U(x) : U \text{ is output by the the NN}\},$$

$$\mathcal{G} = \{\hat{P}(x) : \hat{P} \text{ is output by the NN}\},$$

$$1 - \mathcal{G} = \{1 - \hat{P}(x) : \hat{P} \text{ is output by the NN}\}.$$

Assumption 1 holds for a wide range of NNs, in particular the one we adopt in the experiments (where we use the ReLU-activated NN to construct $\psi_i$, $i = 1, 2, 3, 4$ ; see Section 5). Our first result is to concretely show that the four NN outputs above, $\mathcal{H}_1$, $\mathcal{H}_2$, $\mathcal{G}$ and $1-\mathcal{G}$, under the ReLU setting, all have finite VC dimensions and thus satisfy Assumption 1.

**Theorem 8** (Restated Theorem 2)**.** *Suppose $\psi_i, i = 1, 2, 3, 4$ are the pre-activated output neurons of the NN in Figure 1 using the ReLU activation function. Then Assumption 1 holds. Moreover, suppose the NN has $W$ parameters and $U$ computation units (nodes). Then $V_0 = O(WU)$.*

*Proof.* First, we look at $L(x)$ and $U(x)$. Note that the class of $\psi_i$ $(i = 1, 2)$ is constructed by a NN with the ReLU activation function. Therefore by Theorem 8 in Bartlett et al. (2019) (see also 6 below),

$$V(\{\psi_1\}) = O(WU) < \infty, \quad V(\{\psi_2\}) = O(WU) < \infty.$$

By Lemma 9.9 (i) in Kosorok (2007), we have

$$V(\mathcal{H}_1) = V(\{\min(\psi_1, \psi_2)\}) \leq V(\{\psi_1\}) + V(\{\psi_2\}) - 1 = O(WU) < \infty.$$

By Lemma 9.9 (ii) in Kosorok (2007), we have

$$V(\mathcal{H}_2) = V(\{\max(\psi_1, \psi_2)\}) \leq V(\{\psi_1\}) + V(\{\psi_2\}) - 1 = O(WU) < \infty.$$

Next, we look at $\hat{P}(x)$ and $1 - \hat{P}(x)$. We add an additional neuron after the layer where $\psi_3$, $\psi_4$ stand. This neuron is defined as $\psi_5 = \psi_3 - \psi_4$ which is a linear combination of $\psi_3$ and $\psi_4$. Note that the class of $\psi_5$ is constructed by a NN with the ReLU activation function and linear activation function (by adding one unit and two parameters in the originial NN). Therefore by Theorem 8 in Bartlett et al. (2019),

$$V(\{\psi_5\}) = O(WU) < \infty$$

By Lemma 9.9 (viii) in Kosorok (2007), we have

$$V(\mathcal{G}) = V(\{\sigma(\psi_5)\}) \leq V(\{\psi_5\}) = O(WU) < \infty.$$

since $\sigma$ is a monotone function. Again, by Lemma 9.9 (viii) in Kosorok (2007), we have

$$V(1 - \mathcal{G}) \leq V(\mathcal{G}) = O(WU) < \infty.$$

since $t \mapsto 1 - t$ is a monotone function. □

We also list some results for other activations here. From these results, and using the same argument as above, we see that Assumption 1 holds similarly for all these activations.

**Lemma 6.** *Suppose the class of functions is constructed by a NN with $W$ parameters and $U$ units with activation functions that are piecewise polynomials with at most $p$ pieces and of degree at most $d$. Then it has VC dimension $O(WU\log((d+1)p))$.*

*Proof.* This is Theorem 8 in Bartlett et al. (2019). □

Note that the activation functions in Lemma 6 include in particular the ReLU activation and linear activation.

**Lemma 7.** *Suppose the class of functions is constructed by a NN with $W$ parameters with binary as well as linear activation function. Then it has VC dimension $O(W^2)$.*

*Proof.* This is Theorem 5 in Sontag (1998). □

**Lemma 8.** *Suppose the class of functions is constructed by a NN with $W$ parameters and $U$ units with activation function that is the standard sigmoid function (except that the output unit being a linear threshold unit). Then it has VC dimension $O(W^2U^2)$.*

*Proof.* This is Theorem 8.13 in Anthony and Bartlett (1999). □

### C.3 Connections among Different Hypothesis Classes

To prove Theorem 3, we need to study several building blocks on the relations between different hypothesis classes. Our first observation is:

**Theorem 9.** *Suppose $V(\mathcal{G}) < +\infty$. Then all of the following classes have VC dimension $\leq V(\mathcal{G})$:*

$$1-\mathcal{G} := \{1-\hat{P}(x) : \hat{P} \textit{ is output by the NN}\}.$$

$$\mathcal{G}' := \log(\mathcal{G}) := \{\log(\hat{P}(x)) : \hat{P} \textit{ is output by the NN}\}.$$

$$\log(1-\mathcal{G}) := \{\log(1-\hat{P}(x)) : \hat{P} \textit{ is output by the NN}\}.$$

*Proof.* The result follows from Lemma 9.9 (viii) in Kosorok (2007) since all of the transformations are monotone functions. □

Our second observation is about

$$\mathcal{F} = \{f(x,y) = I_{y\in[L(x),U(x)]} : L, U \text{ are output by the NN}\}.$$

Note that the domain of functions in $\mathcal{F}$ is different from the domain of functions in $\mathcal{H}_i$ $(i = 1, 2)$ as it includes the outcome space. Below we derive a result that connects the VC dimension of $\mathcal{H}_i$ with that of $\mathcal{F}$.

**Theorem 10.** *Suppose $V(\mathcal{H}_i) \leq V_0$ $(i = 1, 2)$. We have that*

$$V(1-\mathcal{F}) \leq V(\mathcal{F}) \leq 10(V_0 - 1) < +\infty$$

*where*

$$1 - \mathcal{F} := \{1 - f(x, y) : f \in \mathcal{F}\}.$$

*Proof.* The first inequality follows from Lemma 9.9 (viii) in Kosorok (2007). We consider the following two classes:

$$\mathcal{F}_1 := \{I_{L(x)\leq t} : L \in \mathcal{H}_1, t \in \mathbb{R}\},$$
$$\mathcal{F}_2 := \{I_{U(x)\geq t} : U \in \mathcal{H}_2, t \in \mathbb{R}\}.$$

Since the functions in $\mathcal{F}_1$ are all indicator functions, by Lemma 5,

$$V(\mathcal{F}_1) = V(\{\{(x,t) : L(x) \leq t\} : L \in \mathcal{H}_1, t \in \mathbb{R}\}).$$

Note that the latter is the VC dimension of the close supergraphs of all functions in $\mathcal{H}_1$. Then by Definition 10 and Lemma 4, we have

$$V(\{\{(x,t) : L(x) \leq t\} : L \in \mathcal{H}_1, t \in \mathbb{R}\}) = V(\mathcal{H}_1)$$

Therefore we have

$$V(\mathcal{F}_1) = V(\mathcal{H}_1) \leq V_0$$

Similarly,

$$V(\mathcal{F}_2) = V(\mathcal{H}_2) \leq V_0$$

Note that we can write

$$I_{y\in[L(x),U(x)]} = I_{L(x)\leq y} I_{U(x)\geq y}$$

By the definition of growth functions,

$$\begin{aligned}\Pi_{\mathcal{F}}(m) :=& \max_{(x_1,y_1),\cdots,(x_m,y_m)} \left|\{(I_{y_1\in[L(x_1),U(x_1)]}, \cdots, I_{y_m\in[L(x_m),U(x_m)]}) : L \in \mathcal{H}_1, U \in \mathcal{H}_2\}\right| \\ \leq& \max_{(x_1,y_1),\cdots,(x_m,y_m)} \left|\{(I_{L(x_1)\leq y_1}, \cdots, I_{L(x_m)\leq y_m}) : L \in \mathcal{H}_1\}\right| \times \\ & \max_{(x_1,y_1),\cdots,(x_m,y_m)} \left|\{(I_{U(x_1)\geq y_1}, \cdots, I_{U(x_m)\geq y_m}) : U \in \mathcal{H}_2\}\right| \\ =& \Pi_{\mathcal{F}_1}(m)\Pi_{\mathcal{F}_2}(m) \\ \leq& \left(\frac{em}{V_0 - 1}\right)^{2(V_0-1)}\end{aligned}$$

for all $m \geq V_0$ where the last inequality is due to the Sauer–Shelah lemma. Taking $m = 10(V_0 - 1)$, we obtain

$$\left(\frac{em}{V_0 - 1}\right)^{2(V_0-1)} = (10e)^{2(V_0-1)} \leq 750^{V_0-1} < 2^m$$

Combining the above inequality, we have

$$\Pi_{\mathcal{F}}(m) < 2^m.$$

This shows that $V(\mathcal{F}) \leq m = 10(V_0 - 1)$. □

### C.4 Proof of Theorem 3

This subsection proves Theorem 3. Recall that

$$\mathcal{F} = \{I_{y \in [L(x), U(x)]} : L, U \text{ are output by the NN}\},$$

$$\mathcal{G} = \{\hat{P}(x) : \hat{P} \text{ is output by the NN}\}.$$

$$\mathcal{G}' := \log(\mathcal{G}) := \{\log(\hat{P}(x)) : \hat{P} \text{ is output by the NN}\}.$$

Let $N(\epsilon, \mathcal{F}, L^2(Q))$ denote the covering number, i.e., the minimal number of balls $\{g : \|g - h\|_{L^2(Q)} < \epsilon\}$ of radius $\epsilon$ needed to cover the set $\mathcal{F}$. We need the following bounds:

**Lemma 9.** *Suppose $\mathcal{F}$ is a class of functions $f : \mathcal{X} \times \mathcal{Y} \to [0, 1]$ with a finite VC dimension $V(\mathcal{F})$. For every $0 < \epsilon < 1$,*

$$\sup_Q \log N(\epsilon, \mathcal{F}, L^2(Q)) \leq K_2 \left(\frac{1}{\epsilon}\right)^{\frac{1}{e}}$$

*where the constant $K_2$ depends on $V(\mathcal{F})$ only.*

*Proof.* It follows from Theorem 2.6.7 in Van der Vaart and Wellner (1996) that there exists a universal constant $K$ such that

$$\sup_Q N(\epsilon, \mathcal{F}, L^2(Q)) \leq K V(\mathcal{F})(16e)^{V(\mathcal{F})} \left(\frac{1}{\epsilon}\right)^{V(\mathcal{F})-1}$$

for any $0 < \epsilon < 1$. Since

$$\left(\frac{1}{\epsilon}\right)^{\frac{1}{e}} \geq \max\left(\log\left(\frac{1}{\epsilon}\right), 1\right), \quad \forall 0 < \epsilon < 1,$$

we have

$$\sup_Q \log N(\epsilon, \mathcal{F}, L^2(Q)) \leq K_3 + (V(\mathcal{F}) - 1)\log\left(\frac{1}{\epsilon}\right) \leq K_2 \left(\frac{1}{\epsilon}\right)^{\frac{1}{e}}$$

where $K_3 := \log(K V(\mathcal{F})(16e)^{V(\mathcal{F})})$ and $K_2 = K_3 + V(\mathcal{F}) - 1$ only depending on $V(\mathcal{F})$. □

We remark that a similar result can also be obtained for the class $1 - \mathcal{F}$ by Theorem 10.

**Lemma 10.** *Suppose $\mathcal{G}$ is a class of functions $\hat{P} : \mathcal{X} \to [0, 1]$ with a finite VC dimension $V(\mathcal{G})$ and $|\log(\hat{P}(x))| \le M$. Let $\mathcal{G}' := \{\log(\hat{P}) : \hat{P} \in \mathcal{G}\}$. Then, for every $0 < \epsilon < 1$,*

$$\sup_Q \log N(\epsilon M, \mathcal{G}', L^2(Q)) \le K_2 \left(\frac{1}{\epsilon}\right)^{\frac{1}{e}}$$

*where the constant $K_2$ depends on $V(\mathcal{G})$ only.*

*Proof.* First note that $\phi(t) := \log(t)$ is a monotone function. Hence $\mathcal{G}' := \{\log(\hat{P}) : \hat{P} \in \mathcal{G}\}$ is a VC-class with VC dimension $\le V(\mathcal{G})$ by Lemma 9.9 (viii) in Kosorok (2007). The rest of the proof is similar to 9. □

We remark that a similar result can also be obtained for the class $\log(1 - \mathcal{G})$ by Theorem 9.

Next we restate Assumption 2:

**Assumption 4** (Restated Assumption 2). *There exists a constant $M < +\infty$ such that $|\log(\hat{P}(x))| \le M$, $|\log(1 - \hat{P}(x))| \le M$ for all $x$ and $\hat{P}$.*

As discussed in Section 4, this is a natural assumption in practice because $\log(\hat{P}(x))$ and $\log(1 - \hat{P}(x))$ are replaced by $\log(\hat{P}(x) + \epsilon)$ and $\log(1 - \hat{P}(x) + \epsilon)$ respectively to avoid explosion when implementing the algorithm. In particular, in our experiments in Section 5, $\epsilon = 0.1^6$ and thus $M = 14$.

We are now ready to prove Theorem 3:

**Theorem 11** (Restated Theorem 3). *Suppose Assumptions 1 and 2 hold. The training data $\mathcal{D} = \{(x_i, y_i),\ i = 1, 2, \cdots, n\}$ where $(x_i, y_i)$ are i.i.d. samples $\sim \pi$. Recall that the (hard) coverage estimator assessment loss is*

$$L_{CA} = -\frac{1}{n} \sum_{i=1}^{n} \Big( f(x_i, y_i) \log(\hat{P}(x_i)) + (1 - f(x_i, y_i)) \log(1 - \hat{P}(x_i)) \Big).$$

*Then for any $t > 0$, we have*

$$\mathbb{P}\left( \sup_{f \in \mathcal{F}, \hat{P} \in \mathcal{G}} |L_{CA} - \mathbb{E}[K_1(X)]| \ge t \right) \le C^* e^{-\frac{nt^2}{16M^2}}$$

*where $C^*$ only depends on $V_0$ in Assumption 1.*

*Proof.* Note that $\mathbb{E}[f(x_i, y_i)|x_i] = A(x_i)$ for any fixed $L$ and $U$. Taking expectation on $L_{CA}$, we have

$$\begin{aligned}
\mathbb{E}[L_{CA}] &= \mathbb{E}\left[\mathbb{E}[L_{CA}|x_1, x_2, \cdots, x_n]\right] \\
&= \mathbb{E}\left[ -\frac{1}{n} \sum_{i=1}^{n} \Big( A(x_i) \log(\hat{P}(x_i)) + (1 - A(x_i)) \log(1 - \hat{P}(x_i)) \Big) \right] \\
&= \mathbb{E}[K_1(X)].
\end{aligned}$$

We consider the first part $A(x)\log(\hat{P}(x))$. The second part can be done using the same argument. Note that by Theorem 9.15 in Kosorok (2007), we have

$$\sup_Q \log N(\epsilon M, \mathcal{F}\cdot\mathcal{G}', L^2(Q)) \leq \sup_Q \log N(\epsilon/2, \mathcal{F}, L^2(Q)) + \sup_Q \log N(\epsilon M/2, \mathcal{G}', L^2(Q)).$$

Consider the class $\frac{1}{2}+\frac{1}{2M}\mathcal{F}\cdot\mathcal{G}' := \{\frac{1}{2}+\frac{1}{2M}(f(x,y)\log(\hat{P}(x))) : f\in\mathcal{F}, \log(\hat{P})\in\mathcal{G}'\}$ which consists of functions taking values in $[0,1]$. We have

$$\begin{aligned}&\sup_Q \log N(\epsilon, \frac{1}{2}+\frac{1}{2M}\mathcal{F}\cdot\mathcal{G}', L^2(Q))\\ =&\sup_Q \log N(2\epsilon M, \mathcal{F}\cdot\mathcal{G}', L^2(Q))\\ \leq&\sup_Q \log N(\epsilon, \mathcal{F}, L^2(Q)) + \sup_Q \log N(\epsilon M, \mathcal{G}', L^2(Q))\\ \leq& K_2\left(\frac{1}{\epsilon}\right)^{1/e}\end{aligned}$$

where the last inequality follows from Lemma 9 and Lemma 10, and $K_2$ only depends on $V(\mathcal{F})$ and $V(\mathcal{G})$. (Recall that we have shown $V(\mathcal{G}')\leq V(\mathcal{G})$ in Lemma 10.) Moreover, by Theorems 9 and 10, we can claim that $K_2$ only depends on $V_0$. This inequality shows that $\frac{1}{2}+\frac{1}{2M}\mathcal{F}\cdot\mathcal{G}'$ satisfies the conditions in Theorem 2.14.10 in Van der Vaart and Wellner (1996) and thus for every $\delta>0$ and $t>0$,

$$\mathbb{P}\left(\sup_{\phi\in\frac{1}{2}+\frac{1}{2M}\mathcal{F}\cdot\mathcal{G}'}\left|\frac{1}{n}\sum_{i=1}^n \phi(x_i,y_i) - \mathbb{E}[\phi(x,y)]\right| \geq t\right) \leq Ce^{D(\sqrt{n}t)^{U+\delta}}e^{-2nt^2}$$

where $U = \frac{\frac{1}{e}(6-\frac{1}{e})}{2+\frac{1}{e}} < 1$ and the constants $C$ and $D$ depend on $K_2$ and $\delta$ only. Let $\delta = 1-U$. Note that

$$-2(\sqrt{n}t)^2 + D(\sqrt{n}t) \leq -(\sqrt{n}t)^2 + (D/2)^2.$$

Hence we have

$$\mathbb{P}\left(\sup_{\phi\in\frac{1}{2}+\frac{1}{2M}\mathcal{F}\cdot\mathcal{G}'}\left|\frac{1}{n}\sum_{i=1}^n \phi(x_i,y_i) - \mathbb{E}[\phi(x,y)]\right| \geq t\right) \leq C^* e^{-nt^2}$$

where $C^*$ only depends on $K_2$, or, only depends on $V_0$.

This shows that

$$\mathbb{P}\left(\sup_{f\in\mathcal{F},\hat{P}\in\mathcal{G}}\left|\frac{1}{n}\sum_{i=1}^n f(x_i,y_i)\log(\hat{P}(x_i)) - \mathbb{E}[A(x)\log(\hat{P}(x))]\right| \geq t\right) \leq C^* e^{-\frac{nt^2}{4M^2}}.$$

A similar result can be established for the second part since the hypothesis classes there have been studied in Theorem 9 and 10:

$$\begin{aligned}&\mathbb{P}\left(\sup_{f\in\mathcal{F},\hat{P}\in\mathcal{G}}\left|\frac{1}{n}\sum_{i=1}^n (1-f(x_i,y_i))\log(1-\hat{P}(x_i)) - \mathbb{E}[(1-A(x))\log(1-\hat{P}(x))]\right| \geq t\right)\\ \leq& C^* e^{-\frac{nt^2}{4M^2}}.\end{aligned}$$

Combining the two parts and noting the following fact:

$$
\begin{aligned}
&\{\sup|\gamma+\beta|\geq t\}\\
\subset&\{\sup|\gamma|+\sup|\beta|\geq t\}\\
\subset&\{\sup|\gamma|\geq \frac{t}{2}\}\cup\{\sup|\beta|\geq \frac{t}{2}\},
\end{aligned}
$$

we conclude that

$$\mathbb{P}\left(\sup_{f\in\mathcal{F},\hat{P}\in\mathcal{G}}|L_{CA}-\mathbb{E}[K_1(x)]|\geq t\right)\leq C^* e^{-\frac{nt^2}{16M^2}}$$

where $C^*$ only depends on $V_0$. □

Lastly, the following corollary explicitly connects our theoretical developments to the experimental setup:

**Corollary 1.** *Suppose the NN is designed as the one specified in the experiments (Section 5). The training data $\mathcal{D}=\{(x_i,y_i),\ i=1,2,\cdots,n\}$ where $(x_i,y_i)$ are i.i.d. samples $\sim\pi$. Then for any $t>0$, we have*

$$\mathbb{P}\left(\sup_{f\in\mathcal{F},\hat{P}\in\mathcal{G}}|L_{CA}-\mathbb{E}[K_1(X)]|\geq t\right)\leq C^* e^{-\frac{nt^2}{16M^2}}.$$

*where $C^*$ only depends on $V_0$ in Assumption 1.*

*Proof.* We note that Assumptions 1 and 2 hold in this case by Theorem 2 and the observation after Assumption 2. So Theorem 3 implies Corollary 1. □

# D Experimental Details and More Results

This section illustrates experimental details and more experimental results from our proposed model.

## D.1 Experimental Details

Table 3 gives a detailed description about the datasets we use. These open-access real-world benchmark regression datasets are widely used for the evaluation of methods in regression tasks (Hernández-Lobato and Adams , 2015; Gal and Ghahramani , 2016; Lakshminarayanan , 2017; Rosenfeld et al. , 2018; Pearce et al. , 2018; Zhu et al. , 2019).

For synthetic datasets, 2000 i.i.d data are generated for each synthetic setting and randomly split into 1000 training data and 1000 testing data. For benchmark datasets, we first do the data normalization and then randomly split 80% data for training and 20% for testing. The choice of

80%/20% split, compared to the 90%/10% split in Pearce et al. (2018), is motivated from the need to increase the test size in order to get a meaningful $ECE$ evaluation. The latter is due to that evaluating $ECE$ requires binning, where using a larger number of bins approximates more closely $CE$, but also requires a larger test size to sustain enough statistical quality for the resulting ECE estimate. This delicate tradeoff motivates us to increase the share of the test set in our split. Following Pearce et al. (2018), our hyper-parameters are selected using the validation set from a random split. Then, they are fixed during the evaluation on other random splits.

As specified in Section 2 (Equation (8)) and Appendix A.4 (Equation (16)), ECE is evaluated based on dividing [0,1] into M sub-intervals. The larger M is, the more precise is in using ECE to approximate CE, the latter being the ideal conditional coverage error estimator. On the other hand, a larger test set size is needed to support the use of a larger M without deteriorating the statistical quality of the ECE. This delicate tradeoff motivates us to increase the share of the test set in our split.

For synthetic datasets, the hyperparameters and corresponding results in Figure 2 are:
(a) $\lambda_1 = 1.7, \lambda_2 = 10^{-5}, \lambda_3 = 1500, CP = 0.95, IW = 0.40, ECE_1 = 0.62\%$.
(b) $\lambda_1 = 1.9, \lambda_2 = 10^{-5}, \lambda_3 = 1000, CP = 0.96, IW = 0.40, ECE_1 = 0.12\%$.
(c) $\lambda_1 = 3.4, \lambda_2 = 10^{-5}, \lambda_3 = 1000, CP = 0.95, IW = 0.50, ECE_1 = 0.65\%$.

For benchmark datasets, the implementation details for baseline algorithms in Table 1 are:

(1) Nearest-neighbors kernel conditional density estimation (NNKCDE). The algorithm is based on Section 2.1 in Dalmasso et al. (2020). We use the same Python code provided by Dalmasso et al. (2020) with the default Gaussian kernel. Two tuning parameters, i.e., the number of nearest neighbors $k$ and the bandwidth $h$ of the smoothing kernel, are chosen in a principled way by minimizing the CDE loss on validation data, the same way as in Dalmasso et al. (2020).

(2) Quantile regression forest (QRF). The algorithm is based on Meinshausen (2006). We use the *RandomForestQuantileRegressor* from the package *scikit-garden* in Python.

(3) Split conformal learning (SCL). The algorithm based on Algorithm 2 in Lei et al. (2018). The regression algorithm inside SCL that we use is a neural network with mean square loss. The neural network has the same structure of hidden layers as in Section 5.

### D.2 Additional Experimental Results

Table 4 gives experimental results for more datasets in addition to Section 5.3.

| Dataset | N | d | Open-access Link |
|---|---|---|---|
| Boston: Boston Housing | 506 | 13 | kaggle.com/c/boston-housing |
| Concrete: Concrete Strength | 1030 | 8 | kaggle.com/aakashphadtare/concrete-data |
| Energy: Energy Efficiency | 768 | 8 | kaggle.com/elikplim/eergy-efficiency-dataset |
| Kin8nm | 8192 | 8 | openml.org/d/189 |
| Plant: Combined Cycle Power Plant | 9568 | 4 | kaggle.com/gova26/airpressure |
| Protein: Protein Structure | 45730 | 9 | networkrepository.com/CASP.php |
| Wine: Red Wine Quality | 1599 | 11 | kaggle.com/uciml/red-wine-quality-cortez-et-al-2009 |
| Yacht: Yacht Hydrodynamics | 308 | 6 | archive.ics.uci.edu/ml/datasets/yacht+hydrodynamics |

Table 3: Full names and details of benchmarking regression datasets. $N$ is the number of samples in the dataset and $d$ is the dimension of the feature vector.

| | | 1-st experiment | | | | 2-nd experiment | | | | 3-rd experiment | | | |
|---|---|---|---|---|---|---|---|---|---|---|---|---|---|
| Dataset | $\lambda_3$ | $\lambda_1$ | $CP$ | $IW$ | $ECE_1$ | $\lambda_1$ | $CP$ | $IW$ | $ECE_1$ | $\lambda_1$ | $CP$ | $IW$ | $ECE_1$ |
| Boston | 1800 | 3.5 | 0.87 | 0.72 | 1.25% | 4.5 | 0.89 | 0.85 | 0.96% | 6.0 | 0.95 | 1.04 | 1.38% |
| Concrete | 1000 | 3.0 | 0.87 | 0.88 | 1.03% | 5.0 | 0.93 | 1.07 | 1.03% | 6.5 | 0.95 | 1.13 | 0.24% |
| Kin8nm | 300 | 2.1 | 0.85 | 0.77 | 1.59% | 2.9 | 0.91 | 0.89 | 0.50% | 3.6 | 0.95 | 1.04 | 1.32% |
| Plant | 700 | 1.6 | 0.85 | 0.63 | 0.86% | 2.4 | 0.91 | 0.75 | 1.15% | 3.3 | 0.95 | 0.85 | 0.38% |
| Protein | 300 | 5.1 | 0.86 | 1.70 | 0.71% | 6.3 | 0.91 | 1.95 | 0.66% | 8.3 | 0.95 | 2.26 | 0.41% |
| Wine | 1100 | 9.0 | 0.85 | 1.59 | 0.98% | 15 | 0.91 | 2.14 | 1.28% | 19 | 0.95 | 2.59 | 0.42% |
| Yacht | 500 | 1.4 | 0.94 | 0.13 | 0.13% | 1.5 | 0.96 | 0.14 | 1.51% | 1.6 | 0.98 | 0.16 | 0.80% |
| Synthetic1 | 1500 | 1.0 | 0.89 | 0.34 | 0.73% | 1.3 | 0.93 | 0.37 | 0.55% | 1.7 | 0.95 | 0.40 | 0.62% |
| Synthetic2 | 1000 | 1.1 | 0.89 | 0.31 | 1.01% | 1.4 | 0.92 | 0.34 | 1.27% | 1.9 | 0.96 | 0.40 | 0.12% |
| Synthetic3 | 1000 | 1.3 | 0.87 | 0.34 | 0.79% | 2.4 | 0.91 | 0.42 | 0.82% | 3.4 | 0.95 | 0.50 | 0.65% |

Table 4: Evaluation metrics of our CaNet on benchmark datasets and synthetic examples with different coverage probabilities.